(Received 10 September 2023, Accepted 21 January 2024, Scheduled 5 February 2024)

Fast Calculations of Vector Electromagnetics in 3D Periodic Structures Based on Multiple Scattering Theory and Broadband Green's Function

Leung Tsang[1], Tien-Hao Liao[2,*], Shurun Tan[3,4,5], Xiaolan Xu[6], Xuyang Bai[3], and Ruoxing Gao[1]

[1]*Radiation Laboratory, Department of Electrical Engineering and Computer Science University of Michigan, Ann Arbor, MI 48109, USA*
[2]*National Taipei University of Technology, Taipei 10608, Taiwan*
[3]*Zhejiang University/University of Illinois at Urbana-Champaign Institute Zhejiang University, Haining 314400, Zhejiang, China*
[4]*State Key Laboratory of Modern Optical Instrumentation College of Information Science and Electronic Engineering Zhejiang University, Hangzhou 310027, China*
[5]*Department of Electrical and Computer Engineering University of Illinois at Urbana-Champaign, Urbana, IL 61801, USA*
[6]*Jet Propulsion Laboratory, California Institute of Technology, Pasadena, CA 91109, USA*

ABSTRACT: We have developed a fast method of using Multiple Scattering Theory-Broadband Green's Function (BBGF-MST) for band field calculations. In this paper, we successfully extended the method to the vector electromagnetic case of 3D periodic structures. In the MST-BBGF approach, the broadband transformation to vector spherical waves for 3D is derived using the Broadband Green's function. The band eigenvalue problem is expressed in terms of the single scatterer T matrix which is independent of the periodic lattice nor the Bloch vector. For the first five bands, the dimension of the KKR eigen equation is merely 6, as 6 vector spherical waves are utilized for the scattered waves. We make extensive comparisons of the results with the commercial software COMSOL in both accuracy and computation efficiency. The CPU requirement on a standard laptop for the MST-BBGF method is merely 0.309 seconds for the first 5 bands. The MST-BBGF method is accurate and is at least two orders of magnitude faster than commercial software COMSOL. In the band field calculations, we employ the approach of extended coefficient to use the low order eigenvector of 6 to extend to 240 vector spherical wave coefficients without the need of recalculating the eigenvalue nor the eigenvector of the KKR equation. The extended coefficients approach gives accurate band field solutions for the entire (0, 0, 0) cell.

1. INTRODUCTION

The calculation of band diagrams and band field solutions is of interest for applications in photonic crystals and topological photonics [1–7]. The plane wave method [1] offers the advantage of a linear eigenvalue problem, but suffers from poor convergence, requiring a large number of plane waves. The finite element method (FEM) [8] and finite difference method (FDM) [9] have also been used, as they readily allow for imposition of Bloch boundary conditions. Both FEM and FDM methods require volumetric discretization of the unit cell. In the case of 3D vector electromagnetic waves, the FEM and FDM will result in large matrix dimensions for the eigenvalue problem. Analytical approximations, such as tight binding approximations, have also been used for vector 3D problems in topological photonics [2].

We have recently combined the Broadband Green's Functions (BBGF) with Multiple Scattering Theory (MST) for efficient band field calculations [10–16]. Multiple scattering theory formulates the multiple scattering of waves among scatterers, and it utilizes the Green's function in terms of translational addition theorem to represent the propagation between the scatterers [17–21]. The MST-BBGF method offers two unique features [10–16]. Firstly, the BBGF method allows for rapid calculations of band diagrams for multiple frequencies, making it a broadband method. Secondly, unlike classical Green's function expansions, the BBGF method exhibits rapid convergence by utilizing imaginary wavenumber extractions [16]. Previously the method was developed for 2D and the scalar waves for 3D [15]. It is important to develop the methodology for vector 3D case as the CPU requirements for vector 3D cases of photonic crystals are demanding in CPU.

The formulation of the band diagram and band field problems can be derived from the multiple scattering theory (MST). The MST was initially developed by Foldy and Lax for random medium and by Korringa for periodic problem. In this paper we follow the equations of Foldy-Lax [17–21] and use the T matrix of a single scatterer [19–21]. The T matrix is independent of the lattice and is also independent of the Bloch vector. Using vector spherical waves, addition theorem, and broadband scalar Green's function in spherical waves, the KKR (Korringa-

* Corresponding author: Tien-Hao Liao (thliao@ntut.edu.tw).

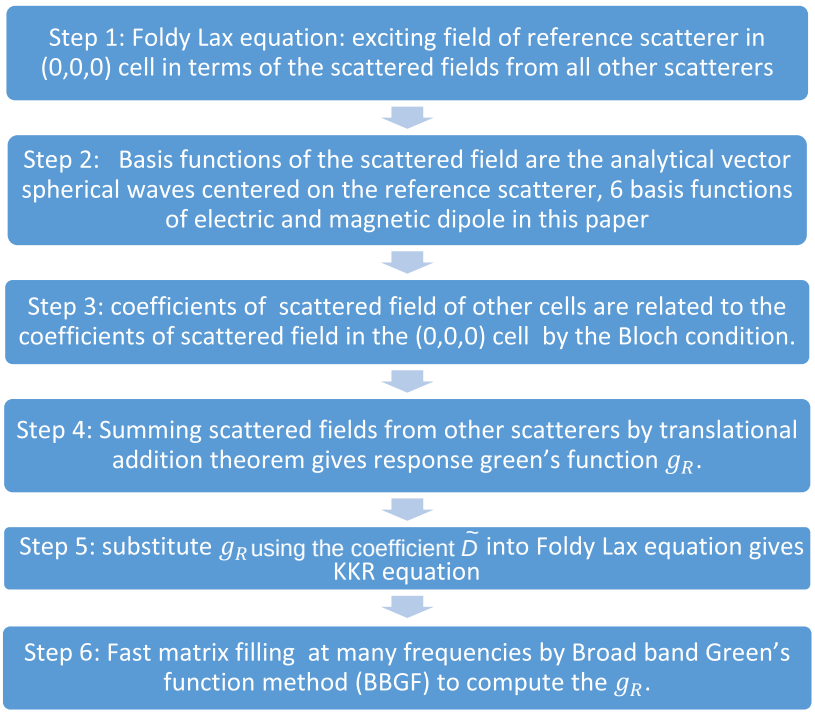

FIGURE 1. Flowchart of MST-BBGF method.

Kohn-Rostoker) [21, 22] eigen-equation is derived. For the first five bands, the dimension of the KKR eigen equation is only 6 as 6 vector spherical waves are sufficient to represent the scattered field around the scatterer. The non-linear search for the band eigen-frequency of the KKR eigen equations facilitated by BBGF as matrix filling can be performed fast using the broad band spherical waves coefficients of the periodic Green's function. The CPU requirement for the MST-BBGF method for a single Bloch vector is merely 0.309 seconds for the first 5 bands on a standard laptop. The Fast MST-BBGF method is several hundred times faster than COMSOL. After the band eigen-frequency is calculated, we perform band field calculations. We develop the extended coefficient approach that extends the low order eigenvector of 6 to 70 and even 240 vector spherical wave coefficients without the need to recalculate the eigen solution. We show that the extended coefficients approach gives accurate band field results for the entire (0, 0, 0) cell.

The organization of this paper is as follows. In Section 2, we derive the KKR equation for the case of vector electromagnetic waves in 3D periodic structures based on the MST of Foldy-Lax (FL). It is shown that only the scalar lattice Green's function, and not the dyadic lattice Green's function, is required for the calculations of the matrix elements of the KKR eigen-equation. In Section 3, we show the fast broadband calculations of the matrix elements for broadband filling by using BBGF. In Section 4, we put the KKR equation in matrix form using the low-dimensional T matrix. The eigen-frequency can be calculated by iterative search over frequency. In Section 5, we show how to use the extended coefficient approach to calculate the extended coefficients of the exciting field and the scattered field. Higher order coefficients can be calculated without the need to re-calculate the KKR eigenfrequency of a larger matrix. In Section 6, the results of this paper are shown for dielectric sphere scatterers giving the T matrices as well as internal field coefficients. In Section 7, we illustrate numerical results of band diagrams and band fields. Extensive comparisons are made with COMSOL in terms of accuracies and CPU requirements. Section 8 concludes the paper. Appendix A and B give respectively the vector spherical harmonics and vector spherical waves [23]. Appendix C gives the derivation of KKR equation using the integral equation approach [24, 25]. Appendix D gives the Huygen's principle applied in the periodic structure to calculate electric field from the surface fields of the scatterer.

2. DERIVATION OF KKR BASED ON FOLDY-LAX (FL) MULTIPLE SCATTERING EQUATIONS

In the derivations of KKR equation, the common procedure is to use integral equations and the lattice Green's function [22, 23, 24, 26]. In this section, we derived the KKR equation based on Foldy-Lax (FL) Multiple Scattering Equations without the use of integral equations [20, 21]. The Foldy-Lax equations have been used for random media with random positions of particles. In this section, the approach is applied to periodic scatterers which is a special case of random media.

The derivations in this paper involve many important ideas, and we summarize them with the flowchart in Figure 1. Readers can correlate the detailed derivation in the following sections to steps in the flowchart. Step 1 and Step 2 show the advantage using scattered waves over exciting waves to formulate the problem. Steps 3∼5 show how KKR equation is constructed among

periodical cells. Step 6 applies BBGF approach to speed up broadband calculations.

Consider N_p particles, centered at $\bar{R}_q$, $q = 1, 2, ..., N_p$. The Foldy-Lax equations state that the exciting electric field of particle q, $\bar{E}^{ex(q)}(\bar{r})$ is the incident wave, $\bar{E}^{inc}(\bar{r})$, plus the scattered field from all particles p, $\bar{E}^{s(p)}(\bar{r})$, except particle q itself [20, 21].

$$\bar{E}^{ex(q)}(\bar{r}) = \bar{E}^{inc}(\bar{r}) + \sum_{p\neq q}^{N_p} \bar{E}^{s(p)}(\bar{r}) \tag{1}$$

For periodic system, we can let the number of particles $N_p = \infty$. The Foldy-Lax equations were put forward by Foldy and Lax heuristically [17, 18]. They can be derived rigorously from Maxwell equations [20].

The vector spherical waves are listed in Appendix B that follow the same notations as [20, 21]. The exciting field of particle q, $\bar{E}^{ex(q)}(\bar{r})$, is expanded in regular (Rg) vector spherical waves $Rg\bar{M}_{mn}$ and $Rg\bar{N}_{mn}$ centered at $\bar{R}_q$. $\bar{E}^{s(p)}(\bar{r})$ is expanded in vector spherical waves $\bar{M}_{mn}$ and $\bar{N}_{mn}$ centered at $\bar{R}_p$.

$$\begin{aligned}\bar{E}^{ex(q)}(\bar{r}) &= \sum_{n,m}\Big[w_{mn}^{(M)(q)} Rg\bar{M}_{mn}\left(k\left(\bar{r}-\bar{R}_q\right)\right)\\ &\quad + w_{mn}^{(N)(q)} Rg\bar{N}_{mn}\left(k\left(\bar{r}-\bar{R}_q\right)\right)\Big]\end{aligned} \tag{2}$$

where $w_{mn}^{(M)(q)}$ and $w_{mn}^{(N)(q)}$ are exciting fields coefficients of particle q.

$$\begin{aligned}\bar{E}^{s(p)}(\bar{r}) &= \sum_{\nu,\mu}\Big[a_{\mu\nu}^{s(M)(p)} \bar{M}_{\mu\nu}\left(k\left(\bar{r}-\bar{R}_p\right)\right)\\ &\quad + a_{\mu\nu}^{s(N)(p)} \bar{N}_{\mu\nu}\left(k\left(\bar{r}-\bar{R}_p\right)\right)\Big]\end{aligned} \tag{3}$$

where $a_{\mu\nu}^{s(M)(p)}$ and $a_{\mu\nu}^{s(N)(p)}$ are scattered field coefficients from particle p.

We substitute (2) and (3) in (1),

$$\begin{aligned}&\sum_{n,m}\Big[w_{mn}^{(M)(q)} Rg\bar{M}_{mn}\left(k\left(\bar{r}-\bar{R}_q\right)\right)\\ &\quad + w_{mn}^{(N)(q)} Rg\bar{N}_{mn}\left(k\left(\bar{r}-\bar{R}_q\right)\right)\Big]\\ &= \bar{E}^{inc}(\bar{r}) + \sum_{p\neq q}^{N_p}\sum_{\nu,\mu}\Big[a_{\mu\nu}^{s(M)(p)} \bar{M}_{\mu\nu}\left(k\left(\bar{r}-\bar{R}_p\right)\right)\\ &\quad + a_{\mu\nu}^{s(N)(p)} \bar{N}_{\mu\nu}\left(k\left(\bar{r}-\bar{R}_p\right)\right)\Big]\end{aligned} \tag{4}$$

We next expand outgoing vector spherical waves from $\bar{R}_p$ in terms of Rg vector spherical waves centered at $\bar{R}_q$.

Since $\bar{r}-\bar{R}_p = \bar{r}-\bar{R}_q+(\bar{R}_q-\bar{R}_p)$ and let $\left|\bar{R}_q-\bar{R}_p\right| > \bar{r}-\bar{R}_q$. From page 535 of [21] for $\bar{r}_0 = \bar{R}_q - \bar{R}_p$ and $\bar{r}' = \bar{r}-\bar{R}_q$,

$$\begin{aligned}&\bar{M}_{\mu\nu}\left(k\left(\bar{r}-\bar{R}_q+\left(\bar{R}_q-\bar{R}_p\right)\right)\right)\\ &= \sum_{n,m}\Big[A_{mn\mu\nu}\left(k\left(\bar{R}_q-\bar{R}_p\right)\right) Rg\bar{M}_{mn}\left(k\left(\bar{r}-\bar{R}_q\right)\right)\\ &\quad + B_{mn\mu\nu}\left(k\left(\bar{R}_q-\bar{R}_p\right)\right) Rg\bar{N}_{mn}\left(k\left(\bar{r}-\bar{R}_q\right)\right)\Big]\end{aligned} \tag{5}$$

$$\begin{aligned}&\bar{N}_{\mu\nu}\left(k\left(\bar{r}-\bar{R}_q+\left(\bar{R}_q-\bar{R}_p\right)\right)\right)\\ &= \sum_{n,m}\Big[B_{mn\mu\nu}\left(k\left(\bar{R}_q-\bar{R}_p\right)\right) Rg\bar{M}_{mn}\left(k\left(\bar{r}-\bar{R}_q\right)\right)\\ &\quad + A_{mn\mu\nu}\left(k\left(\bar{R}_q-\bar{R}_p\right)\right) Rg\bar{N}_{mn}\left(k\left(\bar{r}-\bar{R}_q\right)\right)\Big]\end{aligned} \tag{6}$$

Express $\bar{E}^{inc}(\bar{r})$ in terms of Rg waves centered at particle q,

$$\begin{aligned}\bar{E}^{inc}(\bar{r}) &= \sum_{n,m}\Big[a_{mn}^{inc(M)(q)} Rg\bar{M}_{mn}\left(k\left(\bar{r}-\bar{R}_q\right)\right)\\ &\quad + a_{mn}^{inc(N)(q)} Rg\bar{N}_{mn}\left(k\left(\bar{r}-\bar{R}_q\right)\right)\Big]\end{aligned} \tag{7}$$

Substitute in Eq. (4)

$$\begin{aligned}&\sum_{n,m}\Big[w_{mn}^{(M)(q)} Rg\bar{M}_{mn}\left(k\left(\bar{r}-\bar{R}_q\right)\right)\\ &\quad + w_{mn}^{(N)(q)} Rg\bar{N}_{mn}\left(k\left(\bar{r}-\bar{R}_q\right)\right)\Big]\\ &= \sum_{n,m}\Big[a_{mn}^{inc(M)(q)} Rg\bar{M}_{mn}\left(k\left(\bar{r}-\bar{R}_q\right)\right)\\ &\quad + a_{mn}^{inc(N)(q)} Rg\bar{N}_{mn}\left(k\left(\bar{r}-\bar{R}_q\right)\right)\Big]\\ &\quad + \sum_{p\neq q}^{N_p}\sum_{\nu,\mu}\Bigg\{a_{\mu\nu}^{s(M)(p)}\sum_{n,m}\\ &\quad \left[\begin{array}{l} A_{mn\mu\nu}\left(k\left(\bar{R}_q-\bar{R}_p\right)\right) Rg\bar{M}_{mn}\left(k\left(\bar{r}-\bar{R}_q\right)\right)\\ +B_{mn\mu\nu}\left(k\left(\bar{R}_q-\bar{R}_p\right)\right) Rg\bar{N}_{mn}\left(k\left(\bar{r}-\bar{R}_q\right)\right)\end{array}\right]\Bigg\}\\ &\quad + \sum_{p\neq q}^{N_p}\sum_{\nu,\mu}\Bigg\{a_{\mu\nu}^{s(N)(p)}\sum_{n,m}\\ &\quad \left[\begin{array}{l} B_{mn\mu\nu}\left(k\left(\bar{R}_q-\bar{R}_p\right)\right) Rg\bar{M}_{mn}\left(k\left(\bar{r}-\bar{R}_q\right)\right)\\ +A_{mn\mu\nu}\left(k\left(\bar{R}_q-\bar{R}_p\right)\right) Rg\bar{N}_{mn}\left(k\left(\bar{r}-\bar{R}_q\right)\right)\end{array}\right]\Bigg\}\end{aligned} \tag{8}$$

In (8), balance coefficient of $Rg\bar{M}_{mn}(k(\bar{r}-\bar{R}_q))$ gives (Equation (10.4.25a) of Reference [21])

$$\begin{aligned}w_{mn}^{(M)(q)} &= a_{mn}^{inc(M)(q)} + \sum_{\nu,\mu}\sum_{p\neq q}^{N_p} A_{mn\mu\nu}\left(k\left(\bar{R}_q-\bar{R}_p\right)\right) a_{\mu\nu}^{s(M)(p)}\\ &\quad + \sum_{\nu,\mu}\sum_{p\neq q}^{N_p} B_{mn\mu\nu}\left(k\left(\bar{R}_q-\bar{R}_p\right)\right) a_{\mu\nu}^{s(N)(p)}\end{aligned} \tag{9}$$

In (8), balance coefficient of $Rg\bar{N}_{mn}(k(\bar{r}-\bar{R}_q))$ gives (Equation (10.4.25b) of Reference [21])

$$w_{mn}^{(N)(q)} = a_{mn}^{inc(N)(q)} + \sum_{\nu,\mu}\sum_{p\neq q}^{N_p} B_{mn\mu\nu}\left(k\left(\bar{R}_q-\bar{R}_p\right)\right) a_{\mu\nu}^{s(M)(p)}$$

$$+\sum_{\nu,\mu}\sum_{p\neq q}^{N_p} A_{mn\mu\nu}\left(k\left(\bar{R}_q-\bar{R}_p\right)\right)a_{\mu\nu}^{s(N)(p)} \quad (10)$$

Consider a 3D periodic structure in Figure 2.

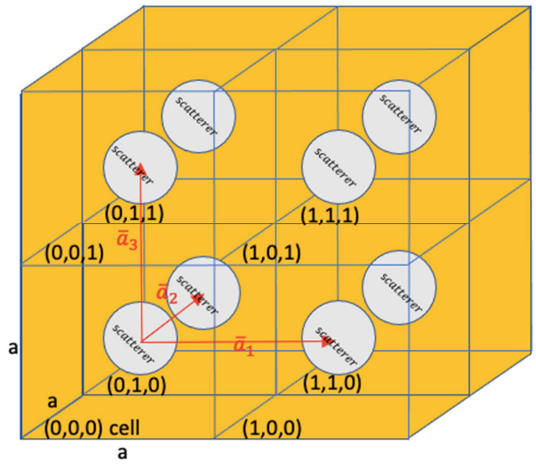

FIGURE 2. The scatterer is of an arbitrary shape and is enclosed by a spherical boundary S_B of radius b about the origin. The origin is the center of the (0, 0, 0) cell. Let S_C be the boundary of the (0, 0, 0) cell.

Let the lattice vector be given by

$$\bar{R}_{mnl}=m\bar{a}_1+n\bar{a}_2+l\bar{a}_3 \quad (11)$$

$m,n,l=0,\pm1,\pm2,...$ where $\bar{a}_1,\bar{a}_2$ and $\bar{a}_3$ are the primitive translation vectors. The cell index is given by (m,n,l). The "center" cell is (0, 0, 0). We also condense the cell index to (m,n,l) to one index "q" or "p" etc. The size(volume) of the cell is $\Omega_0=\bar{a}_1\times\bar{a}_2\cdot\bar{a}_3$. The reciprocal lattice vectors are

$$\bar{G}_{mnl}=m\bar{b}_1+n\bar{b}_2+l\bar{b}_3 \quad (12)$$

$m,n,l=0,\pm1,\pm2,...$ where

$$\begin{aligned}\bar{b}_1 &= 2\pi\frac{\bar{a}_2\times\bar{a}_3}{\Omega_0}\\ \bar{b}_2 &= 2\pi\frac{\bar{a}_3\times\bar{a}_1}{\Omega_0}\\ \bar{b}_3 &= 2\pi\frac{\bar{a}_1\times\bar{a}_2}{\Omega_0}\end{aligned} \quad (13)$$

Let $\bar{k}_i$ be a wave vector in the first Brillouin zone

$$\bar{k}_i=\beta_1\bar{b}_1+\beta_2\bar{b}_2+\beta_3\bar{b}_3 \quad -\frac{1}{2}\le\beta_1,\,\beta_2,\,\beta_3\le\frac{1}{2} \quad (14)$$

We apply the general Foldy-Lax MST of (9) and (10) to the special case of 3D periodic structure. For band solutions, there are no incident waves

$$a_{mn}^{inc(M)(q)}=a_{mn}^{inc(N)(q)}=0 \quad (15)$$

The Bloch condition relates scattered field and exciting field coefficients to the center cell (0, 0, 0) through the Bloch phase shift of $\exp(i\bar{k}_i\cdot\bar{R}_q)$ and $\exp(i\bar{k}_i\cdot\bar{R}_p)$. Thus,

$$\begin{aligned}w_{mn}^{(M)(q)} &= w_{mn}^{(M)}\exp\left(i\bar{k}_i\cdot\bar{R}_q\right) \quad (16)\\ a_{mn}^{s(M)(p)} &= a_{mn}^{s(M)}\exp\left(i\bar{k}_i\cdot\bar{R}_p\right)\\ a_{mn}^{s(N)(p)} &= a_{mn}^{s(N)}\exp\left(i\bar{k}_i\cdot\bar{R}_p\right) \quad (17)\end{aligned}$$

where $w_{mn}^{(M)}$, $w_{mn}^{(N)}$, $a_{mn}^{s(M)}$, and $a_{mn}^{s(N)}$ are the coefficients in the center cell (0, 0, 0). Since the number of particles is infinite in the periodic system, there is no loss of generality to set the particle q to be in the center cell (0, 0, 0), so that $\bar{R}_q=0$. Substitute (15), (16) and (17) in (9) and (10),

$$\begin{aligned}w_{mn}^{(M)} &= \sum_{\nu,\mu} d_{mn\mu\nu}^{(A)}\left(k,\bar{k}_i\right)a_{\mu\nu}^{s(M)}\\ &\quad+\sum_{\nu,\mu} d_{mn\mu\nu}^{(B)}\left(k,\bar{k}_i\right)a_{\mu\nu}^{s(N)} \quad (18)\\ w_{mn}^{(N)} &= \sum_{\nu,\mu} d_{mn\mu\nu}^{(B)}\left(k,\bar{k}_i\right)a_{\mu\nu}^{s(M)}\\ &\quad+\sum_{\nu,\mu} d_{mn\mu\nu}^{(A)}\left(k,\bar{k}_i\right)a_{\mu\nu}^{s(N)} \quad (19)\end{aligned}$$

where

$$d_{mn\mu\nu}^{(A)}(k,\bar{k}_i)=\sum_{\bar{R}_p\neq(0,0,0)} A_{mn\mu\nu}(-k\bar{R}_p)\exp(i\bar{k}_i\cdot\bar{R}_p) \quad (20)$$

$$d_{mn\mu\nu}^{(B)}(k,\bar{k}_i)=\sum_{\bar{R}_p\neq(0,0,0)} B_{mn\mu\nu}(-k\bar{R}_p)\exp(i\bar{k}_i\cdot\bar{R}_p) \quad (21)$$

Eqs. (18) and (19) are the KKR equations for the band eigenvalue problem. The KKR equations need to be solved by searching for the frequency eigenvalue which is a nonlinear search. To simplify and solve the problem fast, we need

(i) fast broadband calculations of $d_{mn\mu\nu}^{(A)}(k,\bar{k}_i)$ and $d_{mn\mu\nu}^{(B)}(k,\bar{k}_i)$ for many frequencies. Both $d_{mn\mu\nu}^{(A)}(k,\bar{k}_i)$ and $d_{mn\mu\nu}^{(B)}(k,\bar{k}_i)$ are oscillatory because of the resonant modes of periodic structures.

(ii) relate the scattered field coefficients $a_{\mu\nu}^{s(M)}$ and $a_{\mu\nu}^{s(N)}$ to the exciting field coefficients $w_{mn}^{(M)}$ and $w_{\nu\mu}^{(N)}$. This can be done through the single scatterer T matrix. The T matrix is independent of the lattice and independent of the Bloch vector $\bar{k}_i$. In the past, the T matrix was limited to spherical scatterer. We recently calculate T matrix of a plant or a tree with complicated structures by using commercial software of FEKO and HFSS [27–30]. Such a method can also be applied to scatterer in photonic crystal and in topological photonics. The T matrix is a smooth function of frequencies because the scatterers in photonic crystals are small to moderate size compared with the wavelengths.

(iii) There is a distinct difference between scattered wave coefficients $a_{\mu\nu}^{s(M)}$, $a_{\mu\nu}^{s(N)}$ and excitation field coefficients, $w_{mn}^{(M)}$, $w_{mn}^{(N)}$. The dimension of scattered field coefficients is dependent on the size of the scatterers. For the numerical results in this paper, it is sufficient to keep only the electric dipole and the magnetic dipole, so that the number of scattered field coefficients is only 6. For the excitation field, it arises from the

scattering of waves from all other scatterers to the scatterer in cell (0, 0, 0). The number of coefficients required depends on the spatial position $\bar{r}$ of the field point relative to the scatterer in the cell (0, 0, 0). When the field point $\bar{r}$ is on the surface of the scatterer of (0, 0, 0), only 6 excitation field coefficients are required giving an eigenvalue problem of 6 by 6. When the spatial position $\bar{r}$ is on the boundary of the cell (0, 0, 0), more excitation coefficients are required and these were calculated by the extended excitation coefficients approach applied to the eigenvector. The extended excitation coefficients approach is discussed in Section 5.

The KKR equations (18) and (19) were derived from Foldy-Lax equations which were proposed heuristically by Foldy and Lax. In Appendix C, by using the integral equation approach, the derived KKR equations are identical to that of (18) and (19).

3. FAST BROADBAND CALCULATIONS OF THE MATRIX ELEMENTS

Combine Eqs. (20) and (21) and Appendix B (B7) and (B8),

$$d^{(A)}_{mn\mu\nu}\left(k,\bar{k}_i\right)=\frac{\gamma_{\mu\nu}}{\gamma_{mn}}\left(-1\right)^m\sum_p\left(-1\right)^p$$

$$a\left(\mu,\nu\left|-m,n\right|p\right)a\left(\nu,n,p\right)\sum_{\bar{R}_s\neq(0,0,0)}$$

$$\exp\left(i\bar{k}_i\cdot\bar{R}_s\right)h_p\left(kR_s\right)Y_p^{\mu-m}\left(\theta_{\bar{R}_s},\phi_{\bar{R}_s}\right)\quad(22)$$

$$d^{(B)}_{mn\mu\nu}\left(k,\bar{k}_i\right)=\frac{\gamma_{\mu\nu}}{\gamma_{mn}}\left(-1\right)^{m+1}\sum_p\left(-1\right)^p$$

$$a\left(\mu,\nu\left|-m,n\right|p\right)b\left(\nu,n,p\right)\sum_{\bar{R}_s\neq(0,0,0)}$$

$$\exp\left(i\bar{k}_i\cdot\bar{R}_s\right)h_p\left(kR_s\right)Y_p^{\mu-m}\left(\theta_{\bar{R}_s},\phi_{\bar{R}_s}\right)\quad(23)$$

where $(\theta_{\bar{R}_s},\phi_{\bar{R}_s})$ are the angles of spherical coordinates associated with $\bar{R}_s$ and $R_s=|\bar{R}_s|$.

Next we relate $\sum_{\bar{R}_s\neq(0,0,0)}\exp(i\bar{k}_i\cdot\bar{R}_s)h_p(kR_s)Y_p^{\mu-m}(\theta_{\bar{R}_s},\phi_{\bar{R}_s})$ to the response Green's function $g_R(k,\bar{k}_i,\bar{r})$.

The response Green's function $g_R(k,\bar{k}_i,\bar{r})$ has the $\bar{r}$ position in cell (0, 0, 0). It is the summation of point sources from other cells into the (0, 0, 0) cell with each point source weighted by the Bloch phase shift $\exp(i\bar{k}_i\cdot\bar{R}_s)$. It is a scalar function, and the dyadic version is not required in the derivations.

$$g_R\left(k,\bar{k}_i,\bar{r}\right)=\sum_{\bar{R}_s\neq(0,0,0)}\exp\left(i\bar{k}_i\cdot\bar{R}_s\right)\frac{\exp\left(i\bar{k}_i\cdot\left(\bar{r}-\bar{R}_s\right)\right)}{4\pi\left|\bar{r}-\bar{R}_s\right|}\quad(24)$$

Since $g_R(k,\bar{k}_i,\bar{r})$ is nonsingular at the origin and is a solution of the scalar wave equation, it can be expanded in scalar *Rg* spherical waves.

$$g_R\left(k,\bar{k}_i,\bar{r}\right)=\sum_{n=0}^{n}\sum_{m=-n}\tilde{D}^{(V)}_{mn}\left(k,\bar{k}_i\right)j_n\left(kr\right)Y_n^{(m)}(\theta,\phi)\quad(25)$$

where $\tilde{D}^{(V)}_{mn}(k,\bar{k}_i)$ are the coefficients of scalar wave expansions and we used superscript (V) to denote the difference from our previous definition in [15]. Form Harrington [31] and Sarabandi [32], we have

$$\frac{\exp\left(i\bar{k}_i\cdot\left(\bar{r}-\bar{R}_s\right)\right)}{4\pi\left|\bar{r}-\bar{R}_s\right|}=\frac{ik}{4\pi}\sum_{n=0}^{\infty}\sum_{m=-n}^{n}\left(-1\right)^m\left(2n+1\right)$$

$$h_n\left(kR_s\right)Y_n^{(-m)}\left(\theta_{\bar{R}_s},\phi_{\bar{R}_s}\right)j_n\left(kr\right)Y_n^{(m)}\left(\theta,\phi\right)\quad(26)$$

Setting (24) and (25) to be equal we obtain

$$\tilde{D}^{(V)}_{mn}\left(k,\bar{k}_i\right)=\frac{ik}{4\pi}\left(-1\right)^m\left(2n+1\right)\sum_{\bar{R}_s\neq(0,0,0)}$$

$$\exp\left(i\bar{k}_i\cdot\bar{R}_s\right)h_n\left(kR_s\right)Y_n^{(-m)}\left(\theta_{\bar{R}_s},\phi_{\bar{R}_s}\right)\quad(27)$$

Then substituting (27) in (22)–(23), we obtain

$$d^{(A)}_{mn\mu\nu}\left(k,\bar{k}_i\right)=\frac{4\pi}{ik}\frac{\gamma_{\mu\nu}}{\gamma_{mn}}\left(-1\right)^{\mu}\sum_{p=0}\left(-1\right)^p$$

$$\frac{a\left(\mu,\nu\left|-m,n\right|p\right)a\left(\nu,n,p\right)}{\left(2p+1\right)}\tilde{D}^{(V)}_{p(m-\mu)}\left(k,\bar{k}_i\right)\quad(28)$$

$$d^{(B)}_{mn\mu\nu}\left(k,\bar{k}_i\right)=\frac{4\pi}{ik}\frac{\gamma_{\mu\nu}}{\gamma_{mn}}\left(-1\right)^{\mu+1}\sum_{p=0}\left(-1\right)^p$$

$$\frac{a\left(\mu,\nu\left|-m,n\right|p\right)b\left(\nu,n,p\right)}{\left(2p+1\right)}\tilde{D}^{(V)}_{p(m-\mu)}\left(k,\bar{k}_i\right)\quad(29)$$

Previously, in [15], we have derived expressions for fast broadband computations of $\tilde{D}_{nm}(k,\bar{k}_i)$ using different definitions of spherical harmonics and associated Legendre polynomials. The conversion to $\tilde{D}^{(V)}_{nm}(k,\bar{k}_i)$ from $\tilde{D}_{nm}(k,\bar{k}_i)$ in this vector 3D paper is

$$\tilde{D}^{(V)}_{nm}\left(k,\bar{k}_i\right)=\left(-1\right)^m\frac{ik}{4\pi}\sqrt{\frac{\left(2n+1\right)\left(n-m\right)!}{\left(n+m\right)!}}\tilde{D}_{nm}\left(k,\bar{k}_i\right)$$

$$n=0,1,2,3,...;\ \ m=0,\pm1,...,\pm n\quad(30)$$

Let

$$A^C\left(\nu,\mu,n,m,p_A\right)=\frac{\gamma_{\mu\nu}}{\gamma_{mn}}\left(-1\right)^m$$

$$a\left(\mu,\nu\left|-m,n\right|p_A\right)a\left(\nu,n,p_A\right)\quad(31)$$

$$B^C\left(\nu,\mu,n,m,p_B\right)=\frac{\gamma_{\mu\nu}}{\gamma_{mn}}\left(-1\right)^{m+1}$$

$$a\left(\mu,\nu\left|-m,n\right|p_B\right)b\left(\nu,n,p_B\right)\quad(32)$$

Then

$$d^{(A)}_{mn\mu\nu}\left(k,\bar{k}_i\right)=\sum_{p_A}A^C\left(\nu,\mu,n,m,p_A\right)\left(-1\right)^{p_A}\left(-1\right)^{(\mu-m)}$$

$$\frac{4\pi}{ik\left(2p_A+1\right)}\tilde{D}^{(V)}_{p_A(m-\mu)}\left(k,\bar{k}_i\right)\quad(33)$$

$$d^{(B)}_{mn\mu\nu}\left(k,\bar{k}_i\right) = \sum_{p_B} B^C\left(\nu,\mu,n,m,p_B\right)(-1)^{p_B}(-1)^{(\mu-m)} \frac{4\pi}{ik\left(2p_B+1\right)}\tilde{D}^{(V)}_{p_B(m-\mu)}\left(k,\bar{k}_i\right) \quad (34)$$

We note the following

a) $d^{(A)}_{mn\mu\nu}(k,\bar{k}_i)$ and $d^{(B)}_{mn\mu\nu}(k,\bar{k}_i)$ are for vector 3D electromagnetic waves and start with $n,\nu=1$.
b) The $\tilde{D}^{(V)}_{pm_p}(k,\bar{k}_i)$ coefficients are generated from scalar 3D waves with the $g_R(k,\bar{k}_i)$ is the Green's function arising from scattering from other particles. We start with $n=0$ in (25). We start with $p=0$ in (28) and (29)
c) The summations over p_A and p_B are over alternate values for given n,ν

$$p_A = |n-\nu|, |n-\nu|+2, ..., n+\nu-2, n+\nu \quad (35)$$
$$p_B = |n-\nu|+1, ..., n+\nu-3, n+\nu-1 \quad (36)$$

4. FAST BROADBAND CALCULATIONS OF MATRIX ELEMENTS OF THE KKR EQUATION

In matrix form, we have

$$\begin{bmatrix} \bar{w}^{(M)} \\ \bar{w}^{(N)} \end{bmatrix} = \begin{bmatrix} \bar{\bar{d}}^{(A)} & \bar{\bar{d}}^{(B)} \\ \bar{\bar{d}}^{(B)} & \bar{\bar{d}}^{(A)} \end{bmatrix} \begin{bmatrix} \bar{a}^{s(M)} \\ \bar{a}^{s(N)} \end{bmatrix} = \begin{bmatrix} \bar{\bar{d}}^{(MM)} & \bar{\bar{d}}^{(MN)} \\ \bar{\bar{d}}^{(NM)} & \bar{\bar{d}}^{(NN)} \end{bmatrix} \begin{bmatrix} \bar{a}^{s(M)} \\ \bar{a}^{s(N)} \end{bmatrix} \quad (37)$$

For vector spherical waves there are two indices, $n=1,2,...$ and $m=-n,-n+1,...,0,1,...,n$. There are also M and N vector wave functions.

We use the following indexing

$$\bar{w}^{(M)} = \begin{bmatrix} w^{(M)}_{-11} \\ w^{(M)}_{01} \\ w^{(M)}_{11} \\ w^{(M)}_{-22} \\ w^{(M)}_{-12} \\ w^{(M)}_{02} \\ w^{(M)}_{12} \\ w^{(M)}_{22} \end{bmatrix}; \quad \bar{w}^{(N)} = \begin{bmatrix} w^{(N)}_{-11} \\ w^{(N)}_{01} \\ w^{(N)}_{11} \\ w^{(N)}_{-22} \\ w^{(N)}_{-12} \\ w^{(N)}_{02} \\ w^{(N)}_{12} \\ w^{(N)}_{22} \end{bmatrix} \quad (38)$$

Let $N_{\max}$ be the maximum n. Then the maximum combined index of $l=(m,n)$ is $L_{\max}=N_{\max}(N_{\max}+2)$.

Thus, if we truncate with $n=1$, dimension of column vector $\bar{w}^{(M)}$ is 3 while if we truncate at $n=2$, dimension of $\bar{w}^{(M)}$ is 8, etc. The indexing of $\bar{w}^{(M)}$, $\bar{w}^{(N)}$, $\bar{a}^{s(M)}$, $\bar{a}^{s(N)}$ column vectors follow the same rule. The indexing of the matrices $\bar{\bar{d}}^{(MM)}$, $\bar{\bar{d}}^{(MN)}$, $\bar{\bar{d}}^{(NM)}$ follow the same rule and are of dimension $L_{\max}\times L_{\max}$.

$$\bar{\bar{d}}^{(MM)} = \bar{\bar{d}}^{(NN)} = \bar{\bar{d}}^{(A)} \quad (39)$$
$$\bar{\bar{d}}^{(MN)} = \bar{\bar{d}}^{(NM)} = \bar{\bar{d}}^{(B)} \quad (40)$$

In a compact form

$$\bar{w} = \bar{\bar{d}}\bar{a}^s \quad (41)$$

where

$$\bar{w} = \begin{bmatrix} \bar{w}^{(M)} \\ \bar{w}^{(N)} \end{bmatrix} \quad (42)$$

$$\bar{a}^s = \begin{bmatrix} \bar{a}^{s(M)} \\ \bar{a}^{s(N)} \end{bmatrix} \quad (43)$$

where

$$\bar{\bar{d}} = \begin{bmatrix} \bar{\bar{d}}^{(A)} & \bar{\bar{d}}^{(B)} \\ \bar{\bar{d}}^{(B)} & \bar{\bar{d}}^{(A)} \end{bmatrix} \quad (44)$$

Because both M and N vector waves are needed, the dimension of the vector 3D KKR equation is $L^V_{\max}=2L_{\max}$. The dimensions of $\bar{w}$ and $\bar{a}^s$ are $L^V_{\max}\times 1$. The dimension of $\bar{\bar{d}}$ is $2L_{\max}\times 2L_{\max}=L^V_{\max}\times L^V_{\max}$.

In MST, the relation between the scattered field coefficients and the exciting field coefficients is via the single scatterer T matrix in vector spherical waves. The T matrix is independent of the lattice nor the Bloch vector. The dimension of the T matrix for photonic crystal problem is small to moderate as the single scatterer has small to moderate size in wavelengths. Let $\bar{\bar{T}}(k)$ be the T matrix in matrix notations. Then

$$\bar{a}^s = \bar{\bar{T}}(k)\bar{w} \quad (45)$$
$$\bar{w} = \bar{\bar{T}}^{-1}(k)\bar{a}^s \quad (46)$$
$$\bar{\bar{T}}^{-1}(k)\bar{a}^s = \bar{\bar{d}}\bar{a}^s \quad (47)$$

The capital $\bar{\bar{T}}(k)$ matrix is of complex values. The KKR equation above is complex. For non-absorptive scatterers, the small $\bar{\bar{t}}$ matrix is used which is real.

Let

$$\bar{\bar{t}} = i\left(\bar{\bar{I}}+\bar{\bar{T}}^{-1}\right) \quad (48)$$

Then we have

$$\bar{\bar{\Lambda}}\bar{a}^s = 0 \quad (49)$$

where

$$\bar{\bar{\Lambda}} = \frac{i}{4}\left(\bar{\bar{d}}+\bar{\bar{I}}\right) - \frac{1}{4}\bar{\bar{t}} \quad (50)$$

Eq. (49) is the KKR equation that includes the T matrix. The dimension of the KKR equation using MST is $L^V_{\max}\times L^V_{\max}$.

The exciting field and scattered fields are truncated with the same $N_{\max}$ for the KKR equation. For the example in this paper, $N_{\max} = 1$, which corresponds to electric dipole and magnetic dipole. The dimension of the KKR equations is 6 by 6. The choice gives the accurate band diagram for the first 5 bands. For the KKR eigen-equation, we choose $N_{\max} = N_L$ so that the dimension of the KKR equation is

$$L_L^V = 2N_L\left(N_L+2\right) \tag{51}$$

The search for band eigenvalue is through nonlinear iterative search. The-normalized frequency is f_N with k corresponding to $k = 2\pi\sqrt{\varepsilon/\varepsilon_0}$ where ε is the permittivity of the background, and ε_0 is the free space permittivity. For a given Bloch vector $\bar{k}_i$, after finding the root of the KKR equation, let the calculated eigenvalue frequency be f_{Ne} and wavenumber k_e. The associated normalized eigenvector is $\bar{a}^s(k_e)$ which is of dimension of $L_L^V \times 1$. The eigenvector $\bar{a}^s(k_e)$ is that of the scatterer of the (0, 0, 0) cell.

5. APPROACH OF EXTENDED COEFFICIENTS

Near the boundary of the scatterer, we use $N_{\max} = N_L$ for both scattered field coefficients and exciting field coefficients. This means

$$a_{\mu\nu}^{s(M)},\ a_{\mu\nu}^{s(N)}\nu \le N_L \tag{52}$$

$$w_{mn}^{(M)},\ w_{mn}^{(N)}n \le N_L \tag{53}$$

Exciting coefficients are also written in terms of scattering coefficients through the summation involving $d_{mn\mu\nu}^{(A)}(k,\bar{k}_i)$ and $d_{mn\mu\nu}^{(B)}(k,\bar{k}_i)$ as Eqs. (18) and (19) to give elements of squared matrix. This was used in solving the KKR eigen-equation. Then the eigensolution of k is calculated, and the eigenvector $a_{\mu\nu}^{s(M)},\ a_{\mu\nu}^{s(N)}\nu \le N_L$ is calculated.

However, to compute the band field solution for the entire (0, 0, 0) cell, we need higher order exciting field coefficients when the distance of the field point from the scatterer increases. This is because the cell can be significantly larger than the scatterer. This means that we still have for the scattered field coefficients

$$a_{\mu\nu}^{s(M)},\ a_{\mu\nu}^{s(N)}\nu \le N_L \tag{54}$$

But for the exciting field coefficients, we need

$$w_{mn}^{(M)},\ w_{mn}^{(N)}n \le N_{sph} \tag{55}$$

with $N_{sph} \ge N_L$.

We still use the same Eq. (18) and Eq. (19) to calculate exciting coefficients from scattering coefficients; however the matrix sizes for $d_{mn\mu\nu}^{(A)}(k,\bar{k}_i)$ and $d_{mn\mu\nu}^{(B)}(k,\bar{k}_i)$ become rectangular due the increase of n.

$$w_{mn}^{(M)} = \sum_{\nu=1}^{N_L}\sum_{\mu=-\nu}^{\nu} d_{mn\mu\nu}^{(A)}\left(k,\bar{k}_i\right)a_{\mu\nu}^{s(M)}$$

$$+\sum_{\nu=1}^{N_L}\sum_{\mu=-\nu}^{\nu} d_{mn\mu\nu}^{(B)}\left(k,\bar{k}_i\right)a_{\mu\nu}^{s(N)};\ 1 \le n \le N_{sph} \tag{56}$$

$$w_{mn}^{(N)} = \sum_{\nu=1}^{N_L}\sum_{\mu=-\nu}^{\nu} d_{mn\mu\nu}^{(B)}\left(k,\bar{k}_i\right)a_{\mu\nu}^{s(M)}$$

$$+\sum_{\nu=1}^{N_L}\sum_{\mu=-\nu}^{\nu} d_{mn\mu\nu}^{(A)}\left(k,\bar{k}_i\right)a_{\mu\nu}^{s(N)};\ 1 \le n \le N_{sph} \tag{57}$$

The governing relations of (54)–(55) are expressed in Eqs. (56)–(57).

Only $d_{mn\mu\nu}^{(A)}(k,\bar{k}_i)$ and $d_{mn\mu\nu}^{(B)}(k,\bar{k}_i)$ have to be recalculated at the eigenvalue k, and not for a lot of k's to get higher order exciting coefficients. We do not need to calculate eigenvalue problem again which is time-consuming for higher order. Once higher order exciting coefficients are done, we can calculate, by using T matrix, the higher order scattering coefficients $a_{\mu\nu}^{s(M)},\ a_{\mu\nu}^{s(N)}N_L+1 \le \nu \le N_{sph}$.

The formulations are general and applicable to scatterers of general shape. We are working on using commercial software such as FEKO and HFSS to extract T matrix for irregular shaped scatterer [27–30]. In the next section, we consider the special case of dielectric spherical scatterers.

6. DIELECTRIC SPHERE

In this paper, the results will be illustrated for dielectric spheres as scatterers. Consider a sphere of permittivity ε_1, with radius b, in a background of permittivity ε. The corresponding wavenumbers are k_1 for the scatterer and k for the background. The T matrix is diagonal for spherical scatterers.

$$T_{mnm'n'}^{(MM)} = T_n^{(M)}\delta_{mm'}\delta_{nn'} \tag{58}$$

$$T_{mnm'n'}^{(NN)} = T_n^{(N)}\delta_{mm'}\delta_{nn'} \tag{59}$$

$$T_{mnm'n'}^{(MN)} = T_n^{(NM)} = 0 \tag{60}$$

where

$$T_n^{(M)}(k) = -\frac{j_n(k_1b)\left(kbj_n(kb)\right)' - j_n(kb)\left(k_1bj_n(k_1b)\right)'}{j_n(k_1b)\left(kbh_n^{(1)}(kb)\right)' - h_n^{(1)}(kb)\left(k_1bj_n(k_1b)\right)'} \tag{61}$$

$$T_n^{(N)}(k) = -\frac{(k_1b)^2 j_n(k_1b)\left(kbj_n(kb)\right)' - (kb)^2 j_n(kb)\left(k_1bj_n(k_1b)\right)'}{(k_1b)^2 j_n(k_1b)\left(kbh_n^{(1)}(kb)\right)' - (kb)^2 h_n^{(1)}(kb)\left(k_1bj_n(k_1b)\right)'} \tag{62}$$

j_n is the spherical Bessel function, and $h_n^{(1)}$ is the spherical Hankel function of the first kind.

Using $\bar{\bar{t}} = i(\bar{\bar{I}} + \bar{\bar{T}}^{-1})$, then

$$t_{mnm'n'}^{(MM)} = t_n^{(M)}\delta_{mm'}\delta_{nn'} \tag{63}$$

$$t_{mnm'n'}^{(NN)} = t_n^{(N)}\delta_{mm'}\delta_{nn'} \tag{64}$$

$$t_{mnm'n'}^{(MN)} = t_n^{(NM)} = 0 \tag{65}$$

$$t_n^{(M)}(k) = \frac{j_n(k_1b)\left(kbn_n(kb)\right)' - n_n(kb)\left(k_1bj_n(k_1b)\right)'}{j_n(k_1b)\left(kbj_n(kb)\right)' - j_n(kb)\left(k_1bj_n(k_1b)\right)'} \tag{66}$$

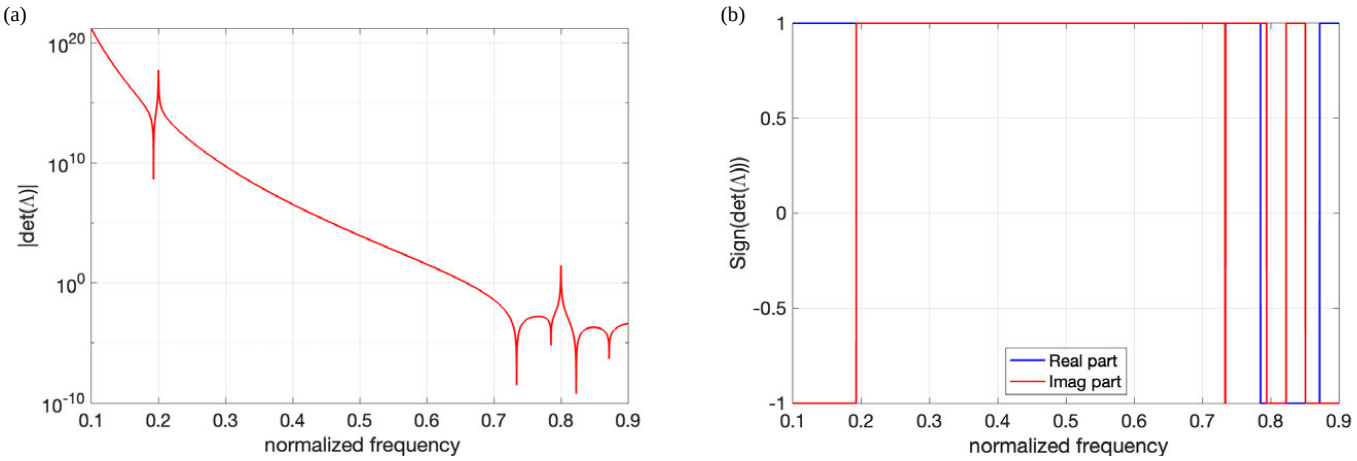

FIGURE 3. Frequency response of (a) absolute value of determinant, (b) sign of determinant.

TABLE 1. CPU simulation time breakdown table from frequency scanning method, bi-section method, and commercial software (COMSOL). (BBGMST on 1.8 GHz Dual-Core Intel Core i5; 8 GB 1600 MHz DDR3); (COMSOL on 2.7 GHz Intel Xeon Gold 6226; 128 GB 2666 MHz DDR4).

Method	Number of bands	Number of frequencies	Set-up (sec)	$\tilde{D}$ and det($\bar{\bar{\Lambda}}$) (sec)	Total cputime (sec)
BBGMST w/Frequency scanning	5	8000	0.165	6.316	6.481
BBGMST w/Bisection	5	109	0.165	0.144	0.309
COMSOL	5	N/A	N/A	N/A	34

$$t_n^{(N)}(k) = \frac{(k_1b)^2 j_n(k_1b)(kbn_n(kb))' - (kb)^2 n_n(kb)(k_1bj_n(k_1b))'}{(k_1b)^2 j_n(k_1b)(kbj_n(kb))' - (kb)^2 j_n(kb)(k_1bj_n(k_1b))'} \quad (67)$$

where n_n is the spherical Neuman function. The advantages of $t_n^{(M)}$ and $t_n^{(N)}$ are that they are real while $T_n^{(M)}$ and $T_n^{(N)}$ are complex.

After the exciting fields are determined, the internal fields are given in terms of vector spherical wave functions and internal field coefficients. The electric field inside the scatterer is,

$$\bar{E}^{int} = \sum_{n=1}^{\infty} \left[c_{mn}^{(M)} Rg\bar{M}_{mn}(k_1\bar{r}) + c_{mn}^{(N)} Rg\bar{N}_{mn}(k_1\bar{r}) \right] \quad (68)$$

where

$$c_{mn}^{(M)} = w_{mn}^{(M)} B_n^{(M)} \quad (69)$$

$$c_{mn}^{(N)} = w_{mn}^{(N)} B_n^{(N)} \quad (70)$$

$$B_n^{(M)} = \frac{i}{kb} \frac{1}{j_n(k_1b)(kbh_n(kb))' - h_n(kb)(k_1bj_n(k_1b))'} \quad (71)$$

$$B_n^{(N)} = \frac{i(k_1b)}{(k_1b)^2 j_n(k_1b)(kbh_n(kb))' - (kb)^2 h_n(kb)(k_1bj_n(k_1b))'} \quad (72)$$

7. NUMERICAL RESULTS

We choose simple cubic lattice (Figure 2) with the lattice constant $a = 1$. The radius of the spherical scatterer is $b = 0.2a$. The background permittivity is $\varepsilon = \varepsilon_0$. The scatterer has permittivity $\varepsilon_p = 8.9\varepsilon_0$.

We shall first illustrate the calculations of the band eigenvalue and band field at the point X in the first Brillouin zone. For the point $\bar{k}_i = 0.2\bar{b}_1$, it means $(\beta_1, \beta_2, \beta_3) = (0.2, 0, 0)$.

We will also illustrate the band diagram for the first 5 bands with $0 \le \beta_1 \le 0.5$, $\beta_2 = \beta_3 = 0$. In the calculations of the broadband spherical wave coefficients $\tilde{D}_{nm}^{(V)}(k, \bar{k}_i)$ with imaginary wavenumber extractions, we use $N_{spa} = 2$, $N_{spe} = 3$, $\xi = \frac{2\pi}{a}$, $R = 0.5a$.

7.1. Eigenvalue and Normalized Eigenvector at $\bar{k}_i = 0.2\bar{b}_1$, $(\beta_1, \beta_2, \beta_3) = (0.2, 0, 0)$

The eigenvalue part is the CPU intensive part of the method because the nonlinear search has to be carried over many frequencies. Based on discussion in the previous section, $N_{\max} = N_L$ are the same for scattered field and exciting field. For $b = 0.2$, we choose a low $N_L = 1$, maximum $n = 1$, for $\tilde{D}_{nm}^{(V)}(k, \bar{k}_i)$. We have 3 pairs of $(n, m) = (1, -1), (1, 0)$, and $(1, 1)$. Thus, the dimension of the eigenvalue equation is 6 when being applied to vector spherical waves $\bar{M}$ and $\bar{N}$, and dimension of the matrix of the KKR eigenvalue equation, $\bar{\bar{\Lambda}}(k)\bar{a}^s = 0$, with $L_{\max} = 3$, $L_{\max}^V = 6$. The normalized frequency is $f_N(k) = \frac{k}{2\pi}\sqrt{\frac{\varepsilon_0}{\varepsilon}}$.

TABLE 2. Scattered field coefficients for $f_{Ne} = 0.7852$.

n	m	l	$a_{mn}^{s(M)}$	$a_{mn}^{s(N)}$
1	−1	1	−0.7071	0
1	0	2	0	0
1	1	3	0.7071	0

TABLE 3. Extended coefficient at $f_{Ne} = 0.7852$ up to $n = 5$: exciting coefficients, $w_{mn}^{(M)}$ and $w_{mn}^{(N)}$, scattering coefficients inside, $c_{mn}^{(M)}$ and $c_{mn}^{(N)}$, and outside the scatterer, $a_{mn}^{s(M)}$ and $a_{mn}^{s(N)}$.

n	m	l	$w_{mn}^{(M)}$	$w_{mn}^{(N)}$	$c_{mn}^{(M)}$	$c_{mn}^{(N)}$	$a_{mn}^{s(M)}$	$a_{mn}^{s(N)}$
1	**−1**	**1**	0.7071 +0.2423i	0	−0.0018 +3.0092i	0	−0.7072 −0.0004i	0
1	**0**	**2**	0	0	0	0	0	0
1	**1**	**3**	−0.7071 −0.2423i	0	0.0018 −3.0092i	0	0.7072 +0.0004i	0
2	**−2**	**4**	−0.1438	0	−0.0416 −0.0003i	0	−0.001i	0
2	**−1**	**5**	0	0	0	0	0	0
2	**0**	**6**	0.1174	0	0.034 +0.0002i	0	0.0008i	0
2	**1**	**7**	0	0	0	0	0	0
2	**2**	**8**	−0.1438	0	−0.0416 −0.0003i	0	−0.001i	0
3	**−3**	**9**	0.4668i	0	0.0322i	0	0	0
3	**−2**	**10**	0	0	0	0	0	0
3	**−1**	**11**	−0.3616i	0	−0.0249i	0	0	0
3	**0**	**12**	0	0	0	0	0	0
3	**1**	**13**	0.3616i	0	0.0249i	0	0	0
3	**2**	**14**	0	0	0	0	0	0
3	**3**	**15**	−0.4668i	0	−0.0322i	0	0	0
4	**−4**	**16**	−0.6286	0	−0.0125	0	0	0
4	**−3**	**17**	0	−0.476	0	−0.0059	0	0
4	**−2**	**18**	0.3521	0	0.007	0	0	0
4	**−1**	**19**	0	−1.2594	0	−0.0155	0	0
4	**0**	**20**	−0.6065	0	−0.012	0	0	0
4	**1**	**21**	0	−1.2594	0	−0.0155	0	0
4	**2**	**22**	0.3521	0	0.007	0	0	0
4	**3**	**23**	0	−0.476	0	−0.0059	0	0
4	**4**	**24**	−0.6286	0	−0.0125	0	0	0
5	**−5**	**25**	−0.137i	0	−0.0008i	0	0	0
5	**−4**	**26**	0	−0.2204i	0	−0.0008i	0	0
5	**−3**	**27**	−0.0737i	0	−0.0004i	0	0	0
5	**−2**	**28**	0	−0.3818i	0	−0.0014i	0	0
5	**−1**	**29**	−0.1759i	0	−0.0011i	0	0	0
5	**0**	**30**	0	0	0	0	0	0
5	**1**	**31**	0.1759i	0	0.0011i	0	0	0
5	**2**	**32**	0	0.3818i	0	0.0014i	0	0
5	**3**	**33**	0.0737i	0	0.0004i	0	0	0
5	**4**	**34**	0	0.2204i	0	0.0008i	0	0
5	**5**	**35**	0.137i	0	0.0008i	0	0	0

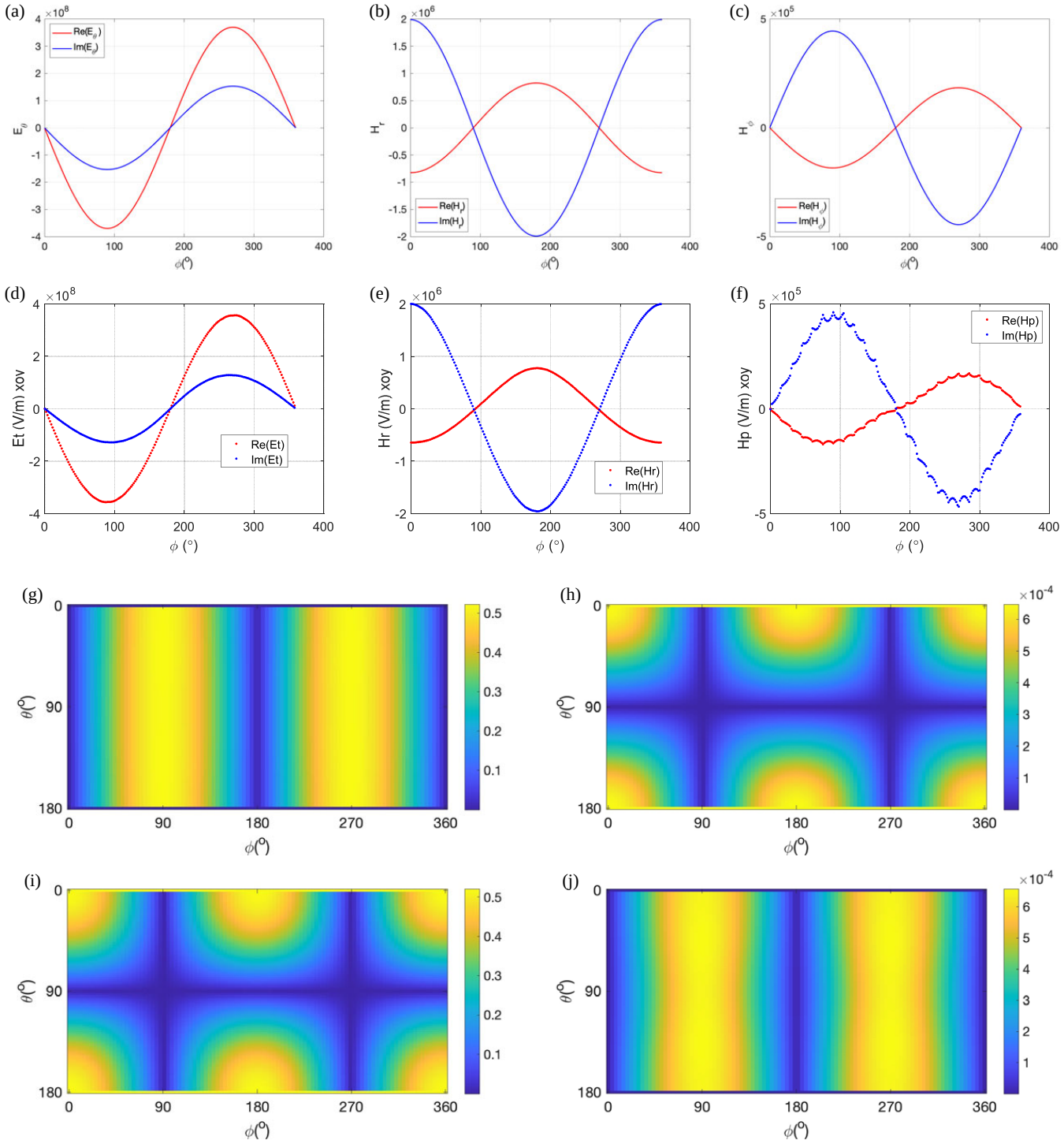

FIGURE 4. Surface fields for band 3. (a) E_θ, (b) H_r, (c) H_ϕ along scatter surface with $\theta = 90^\circ$ from MST-BBGF method, (d) E_θ, (e) H_r, (f) H_ϕ along scatter surface with $\theta = 90^\circ$ from COMSOL; tangential field from MST-BBGF, (g) E_θ, (h) H_θ, (i) E_ϕ, (j) H_ϕ.

Figure 3 shows frequency response of the determinant. Figure 3(a) shows the absolute value of the determinant. It shows 5 zeros within $f_N = 0.1 \sim 0.9$ which corresponds to the first 5 eigenvalues. In Figure 3(b), we look into the sign of the determinant. A tiny imaginary part is added to ξ, $2\pi/a + 0.000001i$, to suppress the oscillation of the sign for the imaginary part of the determinant. We correlate these two figures and we notice where the eigen-values appear:

a) the roots happen with the sign change of real part, and they are non-degenerate.

b) the roots lie within the places when the sign change of imaginary part. However, a further check of whether they are local minimum is needed to determine a real root. These roots found through the sign of imaginary part change are degenerate, and they come in pairs.

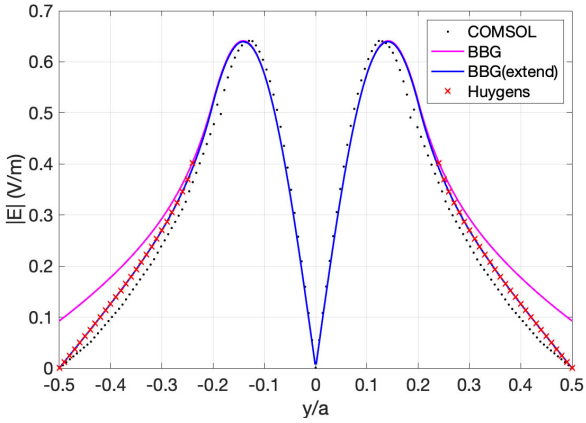

FIGURE 5. Electric field of band 3 ($f_n = 0.7852$) along y-axis.

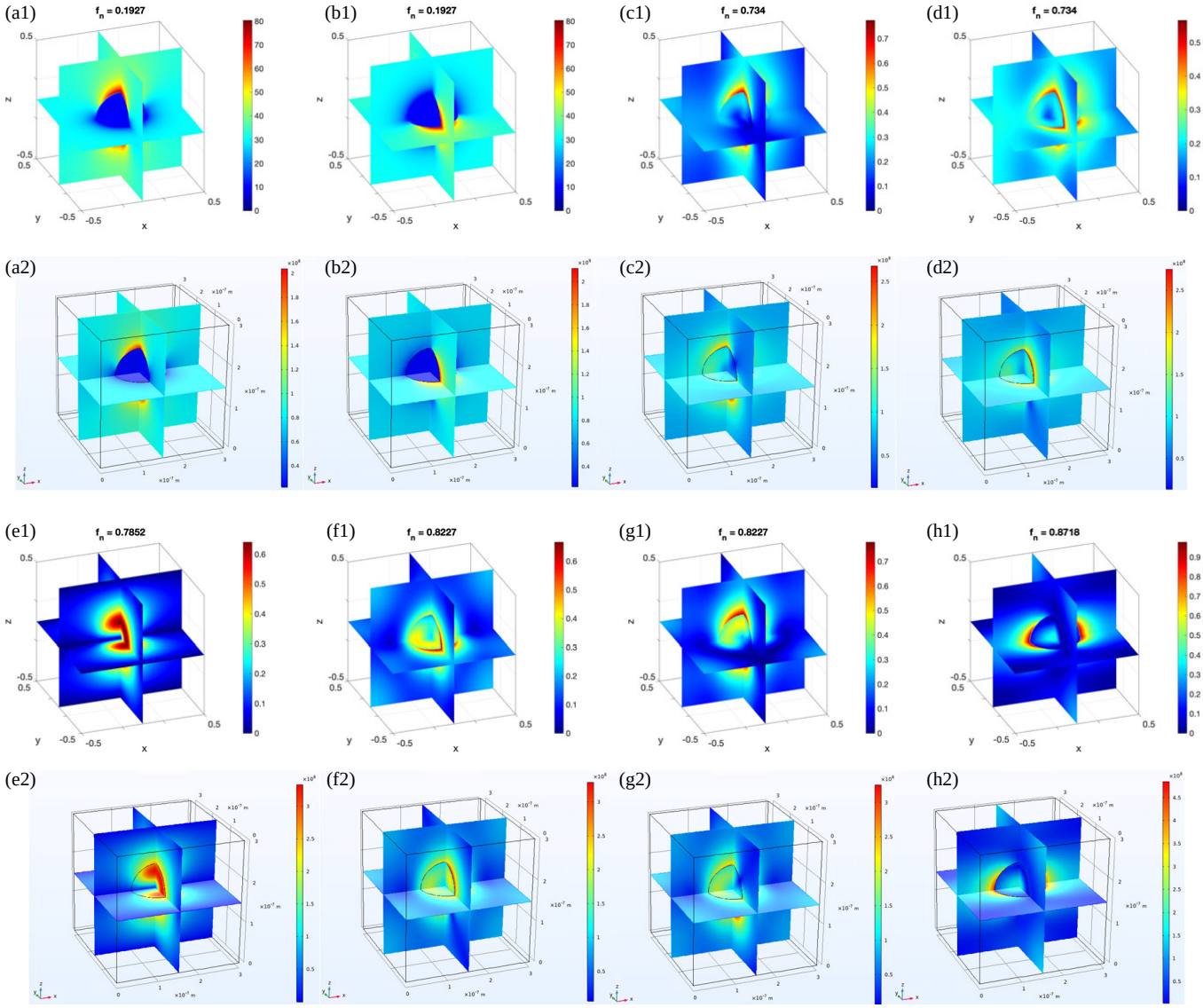

FIGURE 6. 3D band field slices in (0, 0, 0) cell, (a1)∼(h1) from MST-BBGF method and (a2)∼(h2) from COMSOL. (a1), (a2) band 1, 1st degenerate ($f_n^{a1} = 0.1927$; $f_n^{a2} = 0.1925$), (b1), (b2) band 1, 2nd degenerate ($f_n^{b1} = 0.1927$; $f_n^{b2} = 0.1925$), (c1), (c2) band 2, 1st degenerate ($f_n^{c1} = 0.734$; $f_n^{c2} = 0.7324$), (d1), (d2) band 2, 2nd degenerate ($f_n^{d1} = 0.734$; $f_n^{d2} = 0.7324$), (e1), (e2) band 3 ($f_n^{e1} = 0.7852$; $f_n^{e2} = 0.7847$), (f1), (f2) band 4, 1st degenerate ($f_n^{f1} = 0.8227$; $f_n^{f2} = 0.8207$), (g1), (g2) band 4, 2nd degenerate ($f_n^{g1} = 0.8227$; $f_n^{g2} = 0.8207$), (h1), (h2) band 5 ($f_n^{h1} = 0.8718$; $f_n^{h2} = 0.8708$).

With these observations, we also perform the bi-section method to locate these eigenvalues from the sign of real and imaginary parts of determinant individually. We then have the first 5 eigenvalues at 0.1927(degenerate), 0.734(degenerate), 0.7852, 0.8227(degenerate), and 0.8718.

Table 1 shows the comparison of simulation time among proposed methods of MST-BBGF and COMSOL commercial software. The frequency scanning approach is compared with the bi-section method in searching for k. The CPU requirement in this paper for the MST-BBGF method is merely 0.309 seconds for the first 5 bands on a standard laptop. The method outperforms commercial software COMSOL which requires 34 secs that was run on a latest desktop/server. Taking account that the desktop server is 10 times faster than the standard laptop, this means that the Fast MST-BBGF method is several hundred times faster than COMSOL. 108060 unknowns or degrees of freedom were solved with COMSOL version 5.5.

We illustrate band field solutions for $f_{Ne} = 0.7852$. The eigenvector for the MST-BBGF method is the scattered field coefficients. The 6 by 1 eigenvector $\begin{bmatrix} \bar{a}^{s(M)} \\ \bar{a}^{s(N)} \end{bmatrix}$ is normalized.

The results of Table 2 show that the band field solution is that of a magnetic dipole since $a_{mn}^{s(N)} = 0$. The advantage of the MST-BBGF method is that the bands are either electric dipole or magnetic dipole or a combination of both. Thus, the MST-BBGF can be regarded as an analytical method as distinct from finite methods of FEM, FDTD and MoM.

7.2. Higher Order Vector Spherical Waves Based on the Approach of Extended Coefficients

After the eigenvalue and eigenvector of the scattered field coefficients are obtained, we calculate the band field solutions for the entire $(0, 0, 0)$ cell using Equations (56) and (57) in the extended coefficients approach. We calculate up to $n = N_{sph} = 10$ with $L_{\max} = 120$. We list the coefficients up to $n = 5$ in Table 3. From the table, it can be seen that based on the extended coefficients approach, the scattered field coefficients remain the same as up to $n = 2$, and the higher order scattered field coefficients, $n > 2$, do not contribute. On the other hand, the contribution of higher order exciting field coefficients to the band field depends on the distance r from the center of the cell (0, 0, 0).

7.3. The Band Field Solution

We next plot the band field solution within the (0, 0, 0) cell in Figure 4. We demonstrate the results for surface field on the surface of the scatterer and 3D fields within the cell. We also perform extensive comparisons against results from COMSOL. First, at the boundary of the scatterer $r = b = 0.2a$, we consider the cut along peripheral of the sphere with $\theta = 90°$. After the complex scaling of the eigenvector, we compare significant surface terms with COMSOL's results for significant surface terms. The results of MST-BBGF agree well with that of COMSOL. We observe that some results from COMSOL suffer from some small oscillation. The size of eigenvalue problem for MST-BBGF is small giving essentially an analytical solution. The simple summation over vector spherical waves gives smooth surface fields. Figure 4 also shows the tangential field along the entire scatterer surface.

In Figure 5, we compare the band fields along the y-axis for the absolute value of electric field. From MST-BBGF method, we show results from $N_L = 1$ which is of lower order. At cell boundary, $y = -0.5, 0.5$, it shows non-zero field. However, after we extend the coefficients for exciting field, the field at the cell boundary becomes zero. The results then are in agreement with what COMSOL's results. This explains why higher order coefficients of the exciting field are required in calculating band field away from the scatterer. Since the surface fields compare well in Figure 4, we further include another band field calculation from Huygen's principle for field outside the scatterer. The results of Huygen's principle show excellent agreement with those from MST-BBGF method. Huygen's principle is implemented using vector Green's theorem which involves lattice dyadic Green's function and its derivative. The method of Huygen's principle is described in Appendix D. In Figure 6, we show the 3D band field slices within the (0, 0, 0) cell for first five bands from MST-BBGF method and COMSOL, respectively. We observe good agreement especially for band 3 and band 5 which are not degenerate. For degenerate bands like band 1, 2, and 4, we also observe quite close similarity.

7.4. Band Diagram

In Figure 7, we plot the band diagram for the first five bands between Γ and X points in the first Brillouin zone for $\beta_2 = \beta_3 = 0$ and $0 \le \beta_1 \le \frac{1}{2}$. The lowest band is close to a straight line near Γ point meaning that an effective permittivity can be derived. The lowest band is that of metamaterials which is a special case of photonic crystal [10, 11]. The entire five bands are in good agreement between MST-BBGF method and COMSOL.

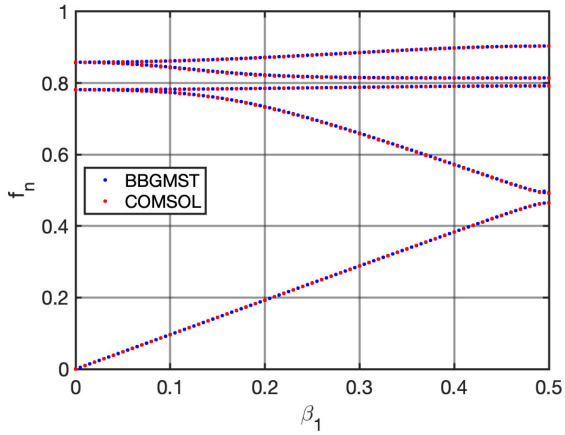

FIGURE 7. Band diagram of first five bands between Γ and X points.

8. CONCLUSIONS

In band diagram calculations, the CEMs (computational electromagnetic methods) have been applied including FDFD/FDTD, FEM, and MoM. In these methods, subsectional

basis functions are used to represent the electromagnetic fields. The band structures in a photonic crystal are results of multiple scattering among the scatterers that are periodically positioned. In this paper, we use a method that is different from CEM, viz. the multiple scattering theory (MST). The basis functions are analytical vector spherical waves of the reference scatterer in the (0, 0, 0) cell which are used to represent the scattered waves. There are only 6 basis functions, so that the unknowns are 6 coefficients. The coefficients in other cells are related to the coefficients of the center cell by the Bloch condition. The band diagram equation, KKR equation, is merely of dimension 6 by 6 for the first 5 bands. To calculate the matrix elements of the KKR matrix equation, the translational addition theorem is used, and the summation over all other scatterers gives the response Green's function g_R. The broad band Green's function method (BBGF) with imaginary wavenumber extraction is used to compute the g_R fast. Using this BBGF method, the matrix elements of the KKR equation are calculated fast for many frequencies so that an iterative search can be readily applied to calculate the band frequency eigenvalues. The efficiency of the MST-BBGF method is shown to be more than two orders of magnitude faster than COMSOL. After the band eigenvalues are determined, the exciting fields and the band field solutions throughout the entire cell are calculated by using the approach of extended coefficients up to 240 vector spherical wave coefficients. In MST, the T matrix is that of an isolated single scatterer which is independent of the lattice and independent of the Bloch vector. For future work of considering irregular shaped scatterer, the T matrix can be precalculated separately using various techniques such as MoM, FEM and FDFD/FDTD, and commercial software such as HFSS, FEKO, and CST in the frequency range of interest and then used for all lattices and Bloch vectors [27–30].

ACKNOWLEDGEMENT

The work of Tsang and Gao were supported by University of Michigan. The work of Liao was supported by National Taipei University of Technology. The work of Tan and Bai were supported by Zhejiang University startup funds and National Natural Science Foundation of China (61901411). The work of Xiaolan Xu was supported by the Jet Propulsion Laboratory of the California Institute of Technology.

APPENDIX A. LEGENDRE POLYNOMINALS AND SPHERICAL HARMONICS

We first define associated Legendre polynomials and spherical harmonics used in this paper as there are several definitions. The associated Legendre polynomial and spherical harmonics are for both positive and negative values of m.

$$P_n^m(x) = \frac{(-1)^m}{2^n n!}\left(1-x^2\right)^{\frac{m}{2}}\frac{d^{n+m}}{dx^{n+m}}\left(x^2-1\right)^n \quad \text{(A1)}$$

$$Y_n^m(\theta,\phi) = P_n^m(\cos\theta)\exp(im\phi) \quad \text{(A2)}$$

with $m = 0, \pm1, ..., \pm n$.

The three vector spherical harmonics are

$$\bar{P}_{mn}(\hat{r}) = \hat{r}Y_n^m(\theta,\phi) \quad \text{(A3)}$$

$$\bar{B}_{mn}(\hat{r}) = \left[\hat{\theta}\frac{dP_n^m(\cos\theta)}{d\theta} + \hat{\phi}\frac{im}{\sin\theta}P_n^m(\cos\theta)\right]e^{im\phi} \quad \text{(A4)}$$

$$\bar{C}_{mn}(\hat{r}) = \left[\hat{\theta}\frac{im}{\sin\theta}P_n^m(\cos\theta) - \hat{\phi}\frac{dP_n^m(\cos\theta)}{d\theta}\right]e^{im\phi} \quad \text{(A5)}$$

The two vector spherical waves are

$$\bar{M}_{mn}(k\bar{r}) = \gamma_{mn}h_n^{(1)}(kr)\bar{C}_{mn}(\hat{r}) \quad \text{(A6)}$$

$$\bar{N}_{mn}(k\bar{r}) = \gamma_{mn}\left[\frac{n(n+1)h_n^{(1)}(kr)}{kr}\bar{P}_{mn}(\hat{r}) + \frac{\left(krh_n^{(1)}(kr)\right)'}{kr}\bar{B}_{mn}(\hat{r})\right] \quad \text{(A7)}$$

with $n = 1, 2, ...$ and $m = 0, \pm1, ..., \pm n$.

Where

$$\gamma_{mn} = \sqrt{\frac{(2n+1)(n-m)!}{4\pi n(n+1)(n+m)!}} \quad \text{(A8)}$$

Since $P_n^m(-x) = (-1)^{n+m}P_n^m(x)$, then

$$Y_n^m(\pi-\theta,\pi+\phi) = (-1)^n Y_n^m(\theta,\phi) \quad \text{(A9)}$$

APPENDIX B. $A_{\mu\nu mn}(k\bar{r}_o)$ AND $B_{\mu\nu mn}(k\bar{r}_o)$

$$A_{\mu\nu mn}(k\bar{r}_0) = \frac{\gamma_{mn}}{\gamma_{\mu\nu}}(-1)^\mu \sum_p a(m,n\,|-\mu,\nu|\,p)\,a(n,\nu,p)\,h_p(kr_0)\,Y_p^{m-\mu}(\theta_0,\phi_0) \quad \text{(B1)}$$

$$B_{\mu\nu mn}(k\bar{r}_0) = \frac{\gamma_{mn}}{\gamma_{\mu\nu}}(-1)^{\mu+1} \sum_p a(m,n|-\mu,\nu|p,p-1)\,b(n,\nu,p)h_p(kr_0)Y_p^{m-\mu}(\theta_0,\phi_0) \quad \text{(B2)}$$

where

$$a(n,\nu,p) = \frac{i^{\nu-n+p}(2\nu+1)}{2\nu(\nu+1)}[\nu(\nu+1)+n(n+1)-p(p+1)] \quad \text{(B3)}$$

$$b(n,\nu,p) = -\frac{i^{\nu-n+p}(2\nu+1)}{2\nu(\nu+1)}[(n+\nu+p+1)(\nu+p-n)(n+p-\nu)(n+\nu-p+1)]^{\frac{1}{2}} \quad \text{(B4)}$$

$$a(m,n\,|\mu,\nu|\,p) = (-1)^{m+\mu}(2p+1)\left[\frac{(n+m)!(\nu+\mu)!(p-m-\mu)!}{(n-m)!(\nu-\mu)!(p+m+\mu)!}\right]^{\frac{1}{2}} \begin{pmatrix} n & \nu & p \\ m & \mu & -(m+\mu) \end{pmatrix}\begin{pmatrix} n & \nu & p \\ 0 & 0 & 0 \end{pmatrix} \quad \text{(B5)}$$

$$a\left(m,n\left|\mu,\nu\right|p,q\right)=(-1)^{m+\mu}\left(2p+1\right)$$

$$\left[\frac{(n+m)!\left(\nu+\mu\right)!\left(p-m-\mu\right)!}{(n-m)!\left(\nu-\mu\right)!\left(p+m+\mu\right)!}\right]^{\frac{1}{2}}$$

$$\left(\begin{array}{ccc} n & \nu & p \\ m & \mu & -(m+\mu) \end{array}\right)\left(\begin{array}{ccc} n & \nu & q \\ 0 & 0 & 0 \end{array}\right) \tag{B6}$$

where $\left(\begin{array}{ccc} n & \nu & p \\ m & \mu & -(m+\mu) \end{array}\right)$ is Wigner 3j symbols. Note that the expression $a(n,\nu,p)$ in (B3) has symmetry in n,ν and p. The expression is different from $a(n,\nu,p)$ in (10.4.16) of [21] which is more complicated. By simplifying (10.4.16) of [21], it can be shown that it is the same as (B3).

For changing sign in the argument, $\bar{r}_0\rightarrow-\bar{r}_0$, $A_{\mu\nu mn}$ and $B_{\mu\nu mn}$ this corresponds to $(\theta_0,\phi_0)\rightarrow(\pi-\theta_0,\pi+\phi_0)$. Then we use $Y_p^{m-\mu}(\pi-\theta_0,\pi+\phi_0)=(-1)^pY_p^{m-\mu}(\theta_0,\phi_0)$.

$$A_{\mu\nu mn}\left(-k\bar{R}_s\right)=\frac{\gamma_{mn}}{\gamma_{\mu\nu}}\left(-1\right)^{\mu}\sum_p\left(-1\right)^p a\left(m,n\left|-\mu,\right.\right.$$

$$\left.\nu\right|p\left)a\left(n,\nu,p\right)h_p\left(kR_s\right)Y_p^{m-\mu}\left(\theta_{R_s},\phi_{R_s}\right)\right. \tag{B7}$$

$$B_{\mu\nu mn}\left(-k\bar{R}_s\right)=\frac{\gamma_{mn}}{\gamma_{\mu\nu}}\left(-1\right)^{\mu+1}\sum_p\left(-1\right)^p a\left(m,n\left|-\mu,\right.\right.$$

$$\left.\nu\right|p,p-1\left)b\left(n,\nu,p\right)h_p\left(kR_s\right)Y_p^{m-\mu}\left(\theta_{R_s},\phi_{R_s}\right)\right. \tag{B8}$$

APPENDIX C. KKR EQUATIONS FROM THE INTEGRAL EQUATION METHOD

The common method of deriving KKR equation is from integral equation. We show the derivations in this section. Let S_{Bj} be the boundary of sphere in periodic cell j. V_{0i} is the region inside S_{Bi}, and V_{1i} is the region outside S_{Bi} in periodic cell i. By using green's theorem, we can derive the following integral equations [23].

$$\sum_j\oint_{S_{Bj}}dS'\left[\overline{\overline{G}}_0\left(\bar{r},\bar{r}'\right)\cdot\hat{n}'\times\nabla'\times\bar{E}_j^s\left(\bar{r}'\right)\right.$$

$$\left.+\nabla\times\overline{\overline{G}}_0\left(\bar{r},\bar{r}'\right)\cdot\hat{n}'\times\bar{E}_j^s\left(\bar{r}'\right)\right]$$

$$=\begin{cases}\bar{E}_{0i}\left(\bar{r}\right)\text{ for }\bar{r}\text{ in }V_{0i}; & i=1,2,3,...\quad\text{(C1)}\\ \bar{E}_i^{ex}\left(\bar{r}\right)\text{ for }\bar{r}\text{ in }V_{1i}; & i=1,2,3,...\quad\text{(C2)}\end{cases}$$

where

$$\bar{E}_{0i}\left(\bar{r}'\right)=\bar{E}_i^{ex}\left(\bar{r}'\right)+\bar{E}_i^s\left(\bar{r}'\right) \tag{C3}$$

Note the integration of the entire cells in written as the summation of each cell.

Exciting field in cell i can be expanded using spherical harmonics with respect to the center $\bar{r}_i$.

$$\bar{E}_i^{ex}\left(\bar{r}\right)=\sum_{m,n}\left[a_{mn}^{(M)(i)}Rg\bar{M}_{mn}\left(k\left(\bar{r}-\bar{r}_i\right)\right)\right.$$

$$\left.+a_{mn}^{(N)(i)}Rg\bar{N}_{mn}\left(k\left(\bar{r}-\bar{r}_i\right)\right)\right] \tag{C4}$$

where $a_{mn}^{(M)(i)}$ and $a_{mn}^{(N)(i)}$ are exciting field coefficients for cell i.

$\overline{\overline{G}}_0(\bar{r},\bar{r}')$ is essentially $\overline{\overline{G}}_0(\bar{r}-\bar{r}')$. We further write it w.r.t. the center of cell $j,\bar{r}_i$.

$$\overline{\overline{G}}_0\left(\bar{r}-\bar{r}'\right)=\overline{\overline{G}}_0\left(\left(\bar{r}-\bar{r}_i\right)-\left(\bar{r}'-\bar{r}_i\right)\right) \tag{C5}$$

For $\bar{r}'$ on S_{Bj} and $\bar{r}$ inside V_{1i}, we have

$$\left|\bar{r}-\bar{r}_i\right|<\left|\bar{r}'-\bar{r}_i\right| \tag{C6}$$

From Equation (2.8.20) in Tsang's volume 1 (page 93) [23], with proper index exchange, we have

$$\overline{\overline{G}}_0\left(\bar{r}-\bar{r}'\right)=ik\sum_{m,n}\left(-1\right)^m$$

$$\left[\begin{array}{l} Rg\bar{M}_{mn}\left(k\left(\bar{r}-\bar{r}_i\right)\right)\bar{M}_{-mn}\left(k\left(\bar{r}'-\bar{r}_i\right)\right) \\ +Rg\bar{N}_{mn}\left(k\left(\bar{r}-\bar{r}_i\right)\right)\bar{N}_{-mn}\left(k\left(\bar{r}'-\bar{r}_i\right)\right)\end{array}\right] \tag{C7}$$

$$\nabla\times\overline{\overline{G}}_0\left(\bar{r}-\bar{r}'\right)=ik^2\sum_{m,n}\left(-1\right)^m$$

$$\left[\begin{array}{l} Rg\bar{N}_{mn}\left(k\left(\bar{r}-\bar{r}_i\right)\right)\bar{M}_{-mn}\left(k\left(\bar{r}'-\bar{r}_i\right)\right) \\ +Rg\bar{M}_{mn}\left(k\left(\bar{r}-\bar{r}_i\right)\right)\bar{N}_{-mn}\left(k\left(\bar{r}'-\bar{r}_i\right)\right)\end{array}\right] \tag{C8}$$

for $|\bar{r}-\bar{r}_i|<|\bar{r}'-\bar{r}_i|$.

We then substitute (C5), (C7), and (C8) into (C2). After balancing $Rg\bar{M}_{mn}(k(\bar{r}-\bar{r}_i))$ and $Rg\bar{N}_{mn}(k(\bar{r}-\bar{r}_i))$, we have

$$\oint_{S_{Bi}}dS'\left[ik\left(-1\right)^m\bar{M}_{mn}\left(k\left(\bar{r}'-\bar{r}_i\right)\right)\cdot\hat{n}'\times\nabla'\times\bar{E}_i^s\left(\bar{r}'\right)\right]$$

$$+\oint_{S_{Bi}}dS'\left[ik^2\left(-1\right)^m\bar{N}_{mn}\left(k\left(\bar{r}'-\bar{r}_i\right)\right)\cdot\hat{n}'\times\bar{E}_i^s\left(\bar{r}'\right)\right]$$

$$+\sum_{j\neq i}\oint_{S_{Bj}}dS'\left[ik\left(-1\right)^m\bar{M}_{mn}\left(k\left(\bar{r}'-\bar{r}_i\right)\right)\right.$$

$$\left.\cdot\hat{n}'\times\nabla'\times\bar{E}_j^s\left(\bar{r}'\right)\right]+\sum_{j\neq i}\oint_{S_{Bj}}dS'\left[ik^2\left(-1\right)^m\right.$$

$$\left.\bar{N}_{mn}\left(k\left(\bar{r}'-\bar{r}_i\right)\right)\cdot\hat{n}'\times\bar{E}_j^s\left(\bar{r}'\right)\right]=a_{-mn}^{(M)(i)} \tag{C9}$$

$$\oint_{S_{Bi}}dS'\left[ik\left(-1\right)^m\bar{N}_{mn}\left(k\left(\bar{r}'-\bar{r}_i\right)\right)\cdot\hat{n}'\times\nabla'\times\bar{E}_i^s\left(\bar{r}'\right)\right]$$

$$+\oint_{S_{Bi}}dS'\left[ik^2\left(-1\right)^m\bar{M}_{mn}\left(k\left(\bar{r}'-\bar{r}_i\right)\right)\cdot\hat{n}'\times\bar{E}_i^s\left(\bar{r}'\right)\right]$$

$$+\sum_{j\neq i}\oint_{S_{Bj}}dS'\left[ik\left(-1\right)^m\bar{N}_{mn}\left(k\left(\bar{r}'-\bar{r}_i\right)\right)\right.$$

$$\left.\cdot\hat{n}'\times\nabla'\times\bar{E}_j^s\left(\bar{r}'\right)\right]+\sum_{j\neq i}\oint_{S_{Bj}}dS'\left[ik^2\left(-1\right)^m\right.$$

$$\left.\bar{M}_{mn}\left(k\left(\bar{r}'-\bar{r}_i\right)\right)\cdot\hat{n}'\times\bar{E}_j^s\left(\bar{r}'\right)\right]=a_{-mn}^{(N)(i)} \tag{C10}$$

Note that we separate the self cell contribution and non-self cell contributions in (C9) and (C10).

Before evaluating the integrals, we first consider the addition theorem of spherical harmonics $\bar{M}_{mn}(k(\bar{r}'-\bar{r}_i))$ and $\bar{N}_{mn}(k(\bar{r}'-\bar{r}_i))$.

From Equations (10.4.10) and (10.4.11) in page 535 of [21], we have for $j \neq i$

$$\bar{M}_{mn}\left(k\left(\bar{r}'-\bar{r}_i\right)\right) = \bar{M}_{mn}\left(k\left(\left(\bar{r}'-\bar{r}_j\right)+\left(\bar{r}_j-\bar{r}_i\right)\right)\right)$$

$$= \sum_{\mu\nu}\left\{A_{\mu\nu mn}\left(k\left(\bar{r}_j-\bar{r}_i\right)\right) Rg\bar{M}_{\mu\nu}\left(k\left(\bar{r}'-\bar{r}_j\right)\right)\right.$$

$$\left.+B_{\mu\nu mn}\left(k\left(\bar{r}_j-\bar{r}_i\right)\right) Rg\bar{N}_{\mu\nu}\left(k\left(\bar{r}'-\bar{r}_j\right)\right)\right\} \quad \text{(C11)}$$

$$\bar{N}_{mn}\left(k\left(\bar{r}'-\bar{r}_i\right)\right) = \bar{N}_{mn}\left(k\left(\left(\bar{r}'-\bar{r}_j\right)+\left(\bar{r}_j-\bar{r}_i\right)\right)\right)$$

$$= \sum_{\mu\nu}\left\{B_{\mu\nu mn}\left(k\left(\bar{r}_j-\bar{r}_i\right)\right) Rg\bar{M}_{\mu\nu}\left(k\left(\bar{r}'-\bar{r}_j\right)\right)\right.$$

$$\left.+A_{\mu\nu mn}\left(k\left(\bar{r}_j-\bar{r}_i\right)\right) Rg\bar{N}_{\mu\nu}\left(k\left(\bar{r}'-\bar{r}_j\right)\right)\right\} \quad \text{(C12)}$$

for $|\bar{r}'-\bar{r}_j| < |\bar{r}_j-\bar{r}_i|$.

Scattered field in cell j can be expanded using spherical harmonics w.r.t. the center $\bar{r}_j$.

$$\bar{E}_j^s\left(\bar{r}'\right) = \sum_{m',n'}\left[a_{m'n'}^{(M)(s)(j)}\bar{M}_{m'n'}\left(k\left(\bar{r}'-\bar{r}_j\right)\right)\right.$$

$$\left.+a_{m'n'}^{(N)(s)(j)}\bar{N}_{m'n'}\left(k\left(\bar{r}'-\bar{r}_j\right)\right)\right] \quad \text{(C13)}$$

$$\nabla'\times\bar{E}_j^s\left(\bar{r}'\right) = k\sum_{m',n'}\left[a_{m'n'}^{(M)(s)(j)}\bar{N}_{m'n'}\left(k\left(\bar{r}'-\bar{r}_j\right)\right)\right.$$

$$\left.+a_{m'n'}^{(N)(s)(j)}\bar{M}_{m'n'}\left(k\left(\bar{r}'-\bar{r}_j\right)\right)\right] \quad \text{(C14)}$$

Now we substitute (C11)∼(C14) into (C9) and (C10) and consider $\hat{n}' = \hat{r}'$.

$$\sum_{j\neq i}\oint_{S_{Bj}} dS'\left[ik^2\left(-1\right)^m\bar{M}_{mn}\left(k\left(\bar{r}'-\bar{r}_i\right)\right)\cdot\hat{n}'\times\bar{E}_j^s\left(\bar{r}'\right)\right]$$

$$= \sum_{j\neq i}\sum_{\nu\mu} ik^2\left(-1\right)^m A_{\mu\nu mn}\left(k\left(\bar{r}_j-\bar{r}_i\right)\right)$$

$$a_{(-\mu)\nu}^{(N)(s)(j)}\left(b^2\left(-1\right)^{\mu+1} j_\nu\left(kb\right)\frac{\left[kbh_\nu^{(1)}\left(kb\right)\right]'}{kb}\right)$$

$$+\sum_{j\neq i}\sum_{\nu\mu}\sum_{m',n'} ik^2\left(-1\right)^m B_{\mu\nu mn}\left(k\left(\bar{r}_j-\bar{r}_i\right)\right)$$

$$a_{(-\mu)\nu}^{(M)(s)(j)}\left(b^2\left(-1\right)^{\mu} h_\nu^{(1)}\left(kb\right)\frac{\left[kbj_\nu\left(kb\right)\right]'}{kb}\right) \quad \text{(C15)}$$

$$\sum_{j\neq i}\oint_{S_{Bj}} dS'\left[ik^2\left(-1\right)^m\bar{N}_{mn}\left(k\left(\bar{r}'-\bar{r}_i\right)\right)\cdot\hat{n}'\times\bar{E}_j^s\left(\bar{r}'\right)\right]$$

$$= \sum_{j\neq i}\sum_{\nu\mu} ik^2\left(-1\right)^m B_{\mu\nu mn}\left(k\left(\bar{r}_j-\bar{r}_i\right)\right)$$

$$a_{(-\mu)\nu}^{(N)(s)(j)}\left(b^2\left(-1\right)^{\mu+1} j_\nu\left(kb\right)\frac{\left[kbh_\nu^{(1)}\left(kb\right)\right]'}{kb}\right)$$

$$+\sum_{j\neq i}\sum_{\nu\mu} ik^2\left(-1\right)^m A_{\mu\nu mn}\left(k\left(\bar{r}_j-\bar{r}_i\right)\right)$$

$$a_{(-\mu)\nu}^{(M)(s)(j)}\left(b^2\left(-1\right)^{\mu} h_\nu^{(1)}\left(kb\right)\frac{\left[kbj_\nu\left(kb\right)\right]'}{kb}\right) \quad \text{(C16)}$$

$$\sum_{j\neq i}\oint_{S_{Bj}} dS'\left[ik\left(-1\right)^m\bar{M}_{mn}\left(k\left(\bar{r}'-\bar{r}_i\right)\right)\cdot\hat{n}'\times\nabla'\right.$$

$$\left.\times\bar{E}_j^s\left(\bar{r}'\right)\right] = \sum_{j\neq i}\sum_{\nu\mu} ik^2\left(-1\right)^m A_{\mu\nu mn}\left(k\left(\bar{r}_j-\bar{r}_i\right)\right)$$

$$a_{(-\mu)\nu}^{(M)(s)(j)}\left(b^2\left(-1\right)^{\mu+1} j_\nu\left(kb\right)\frac{\left[kbh_\nu^{(1)}\left(kb\right)\right]'}{kb}\right)$$

$$+\sum_{j\neq i}\sum_{\nu\mu} ik^2\left(-1\right)^m B_{\mu\nu mn}\left(k\left(\bar{r}_j-\bar{r}_i\right)\right)$$

$$a_{(-\mu)\nu}^{(N)(s)(j)}\left(b^2\left(-1\right)^{\mu} h_\nu^{(1)}\left(kb\right)\frac{\left[kbj_\nu\left(kb\right)\right]'}{kb}\right) \quad \text{(C17)}$$

$$\sum_{j\neq i}\oint_{S_{Bj}} dS'\left[ik\left(-1\right)^m\bar{N}_{mn}\left(k\left(\bar{r}'-\bar{r}_i\right)\right)\cdot\hat{n}'\times\nabla'\right.$$

$$\left.\times\bar{E}_j^s\left(\bar{r}'\right)\right] = \sum_{j\neq i}\sum_{\nu\mu} ik^2\left(-1\right)^m B_{\mu\nu mn}\left(k\left(\bar{r}_j-\bar{r}_i\right)\right)$$

$$a_{(-\mu)\nu}^{(M)(s)(j)}\left(b^2\left(-1\right)^{\mu+1} j_\nu(kb)\frac{\left[kbh_\nu^{(1)}\left(kb\right)\right]'}{kb}\right)$$

$$+\sum_{j\neq i}\sum_{\nu\mu} ik^2\left(-1\right)^m A_{\mu\nu mn}\left(k\left(\bar{r}_j-\bar{r}_i\right)\right)$$

$$a_{(-\mu)\nu}^{(N)(s)(j)}\left(b^2\left(-1\right)^{\mu} h_\nu^{(1)}\left(kb\right)\frac{\left[kbj_\nu\left(kb\right)\right]'}{kb}\right) \quad \text{(C18)}$$

Among these integrals, many of sub-integrals are zero because of the orthogonality from Eq. (1.4.52) [23].

$$\int_0^\pi d\theta\sin\theta\int_0^{2\pi} d\phi\bar{V}_{mn}^{(\alpha)}\left(\theta,\phi\right)\bar{V}_{-m'n'}^{(\beta)}\left(\theta,\phi\right)$$

$$= \delta_{\alpha\beta}\delta_{mm'}\delta_{nn'}z_{\alpha mn} \quad \text{(C19)}$$

where $\bar{V}_{mn}$ is among $\bar{P}_{mn}, \bar{B}_{mn}, \bar{C}_{mn}$. $z_{\alpha mn}$ is the normalization coefficient. Note that spherical harmonics are written using $\bar{P}_{mn}, \bar{B}_{mn}, \bar{C}_{mn}$ from Eqs. (1.4.56) and (1.4.57) from [23].

Substitute (C15)∼(C18) into (C9) and (C10).

$$\sum_{j\neq i}\sum_{\nu\mu} ik^2\left(-1\right)^m A_{\mu\nu mn}\left(k\left(\bar{r}_j-\bar{r}_i\right)\right) a_{(-\mu)\nu}^{(M)(s)(j)} b^2\left(-1\right)^{\mu}$$

$$\left(-\frac{i}{k^2b^2}\right)+\sum_{j\neq i}\sum_{\nu\mu}ik^2\left(-1\right)^m B_{\mu\nu mn}\left(k\left(\bar{r}_j-\bar{r}_i\right)\right)$$

$$a_{(-\mu)\nu}^{(N)(s)(j)}b^2\left(-1\right)^\mu\left(-\frac{i}{k^2b^2}\right)=a_{-mn}^{(M)(i)} \tag{C20}$$

$$\sum_{j\neq i}\sum_{\nu\mu}ik^2\left(-1\right)^m B_{\mu\nu mn}\left(k\left(\bar{r}_j-\bar{r}_i\right)\right)a_{(-\mu)\nu}^{(M)(s)(j)}b^2\left(-1\right)^\mu$$

$$\left(-\frac{i}{k^2b^2}\right)+\sum_{j\neq i}\sum_{\nu\mu}ik^2\left(-1\right)^m A_{\mu\nu mn}\left(k\left(\bar{r}_j-\bar{r}_i\right)\right)$$

$$a_{(-\mu)\nu}^{(N)(s)(j)}b^2\left(-1\right)^\mu\left(-\frac{i}{k^2b^2}\right)=a_{-mn}^{(N)(i)} \tag{C21}$$

Note that the Wronskian is applied.

$$j_n'\left(\omega\right)h_n^{(1)}\left(\omega\right)-j_n\left(\omega\right)h_n^{(1)'}\left(\omega\right)=-\frac{i}{\omega^2} \tag{C22}$$

Also, for $j=i$ in (C9) and (C10), they are all zero.

We further simplify and arrange in the indices in (C20) and (C21).

$$\begin{aligned}a_{-mn}^{(M)(i)} &= \sum_{j\neq i}\sum_{\nu\mu}\Big[A_{\mu\nu mn}\left(k\left(\bar{r}_i-\bar{r}_j\right)\right)a_{\mu\nu}^{(M)(s)(j)}\\ &\quad +B_{\mu\nu mn}\left(k\left(\bar{r}_i-\bar{r}_j\right)\right)a_{\mu\nu}^{(N)(s)(j)}\Big]\end{aligned} \tag{C23}$$

$$\begin{aligned}a_{-mn}^{(N)(i)} &= \sum_{j\neq i}\sum_{\nu\mu}\Big[B_{\mu\nu mn}\left(k\left(\bar{r}_i-\bar{r}_j\right)\right)a_{\mu\nu}^{(M)(s)(j)}\\ &\quad +A_{\mu\nu mn}\left(k\left(\bar{r}_i-\bar{r}_j\right)\right)a_{\mu\nu}^{(N)(s)(j)}\Big]\end{aligned} \tag{C24}$$

(C23) and (C24) show the same equations as (9) and (10) considering no incident field. This means that the rest of the derivation for KKR equations is the same, (11)∼(18). The derivation in this appendix shows that starting from integral equation (IE) method we end up with the same KKR equations as those from Foldy-Lax MST equations. The multiple scattering concept of Foldy-Lax can be directly applied to start the derivation for KKR. This dramatically saves the derivation, and furthermore the embedded idea of multiple scattering within periodical cells is also clearer.

APPENDIX D. HUYGEN'S PRICIPLES APPLIED USING PERIODIC DYADIC GREEN'S FUNCTIONS

For MST-BBGF, the matching of boundary conditions is not on the surface of the scatterer but on the surface of the enclosing sphere using the derived T matrix coefficients of the scatterer. The surface fields on the spherical surface are essentially analytical. Thus, it is also convenient to use the surface fields and Huygen's principle to derive the band fields everywhere outside the circumscribing sphere. In this section, we derive the equations of the Huygen's principle. Consider a periodic lattice and let the lattice constant be a. Let the cells be labeled as (m,n,l). All the cells have the same scatterer placed in a background medium. Consider the (0, 0, 0) cell, the scatterer can be of irregular shape and is enclosed by a circular boundary S_B of radius b. Let S_C be the boundary of the (0, 0, 0) cell. We use V_1 to denote region inside S_B and V_0 be the region outside the scatterer but within the cell (0, 0, 0). Let $\bar{E}$ be the electric field of the vector wave function in V_0. It satisfies the wave equation.

Apply vector Green's theorem from [23],

$$\begin{aligned}&\int_V d\bar{r}\left(\bar{P}\cdot\nabla\times\nabla\times\bar{Q}-\bar{Q}\cdot\nabla\times\nabla\times\bar{P}\right)\\ &= \oint dS\hat{n}\cdot\left(\bar{Q}\times\nabla\times\bar{P}-\bar{P}\times\nabla\times\bar{Q}\right)\end{aligned} \tag{D1}$$

where $\hat{n}$ is outward normal.

Let

$$\bar{P} = \bar{E}\left(\bar{r}'\right) \tag{D2}$$

$$\bar{Q} = \overline{\overline{G}}_0\left(k,\bar{r},\bar{r}'\right)\cdot\bar{c} \tag{D3}$$

$\overline{\overline{G}}_0(k,\bar{r},\bar{r}')$ is free space dyadic Green's function and $\bar{c}$ is arbitrary constant vector.

$$\begin{aligned}&\sum_\sigma\oint_{S_{B\sigma}}dS'\Big[\overline{\overline{G}}_0\left(\bar{r},\bar{r}'\right)\cdot\hat{n}'\times\nabla'\times\bar{E}\left(\bar{r}'\right)\\ &+\nabla\times\overline{\overline{G}}_0\left(\bar{r},\bar{r}'\right)\cdot\hat{n}'\times\bar{E}\left(\bar{r}'\right)\Big]\\ &= \bar{E}\left(\bar{r}\right)\ \text{for}\ \bar{r}\ \text{in}\ V_0\ \text{of}\ (0,\,0,\,0)\\ &= 0\ \text{for}\ \bar{r}\ \text{in}\ V_1\ \text{of}\ (0,0,0)\end{aligned} \tag{D4}$$

where $S_{B\sigma}$ is the circular boundary of scatterer in cell σ.

D.1. Translate $\oint_{S_{B\sigma}}$ to (0, 0, 0) Cell

$$\bar{r}'=\bar{r}''+\bar{R}_\sigma \tag{D5}$$

$\bar{r}'$ on $S_{B\sigma}$ means $\bar{r}''$ on $S_{B\sigma}$ of (0, 0, 0), and $\bar{R}_\sigma$ is the distance between center of cell σ and the origin.

$$\begin{aligned}&\sum_\sigma\oint_{S_{B\sigma}}dS''\Big[\overline{\overline{G}}_0\left(\bar{r},\bar{r}''+\bar{R}_\sigma\right)\cdot\hat{n}''\times\nabla''\times\bar{E}\left(\bar{r}''+\bar{R}_\sigma\right)\\ &+\nabla\times\overline{\overline{G}}_0\left(\bar{r},\bar{r}''+\bar{R}_\sigma\right)\cdot\hat{n}''\times\bar{E}\left(\bar{r}''+\bar{R}_\sigma\right)\Big]\\ &= \bar{E}\left(\bar{r}\right)\ \text{for}\ \bar{r}\ \text{in}\ V_0\ \text{of}\ (0,0,0)\\ &= 0\ \text{for}\ \bar{r}\ \text{in}\ V_1\ \text{of}\ (0,0,0)\end{aligned} \tag{D6}$$

D.2. Bloch's Theorem

The Bloch's theorem is applied to represent electric field using phase shifts between cell centers.

$$\bar{E}\left(\bar{r}''+\bar{R}_\sigma\right)=\bar{E}\left(\bar{r}''\right)\exp\left(i\bar{k}_i\cdot\bar{R}_\sigma\right) \tag{D7}$$

$$\oint_{S_B} dS'' \left[\sum_{\sigma} \overline{\overline{G}}_0 \left(\bar{r}, \bar{r}'' + \bar{R}_\sigma \right) \exp\left(i\bar{k}_i \cdot \bar{R}_\sigma \right) \cdot \hat{n}'' \times \nabla'' \right.$$

$$\left. \times \bar{E}\left(\bar{r}'' \right) + \nabla \times \left(\overline{\overline{G}}_0 \left(\bar{r}, \bar{r}'' + \bar{R}_\sigma \right) \exp\left(i\bar{k}_i \cdot \bar{R}_\sigma \right) \right) \cdot \hat{n}'' \right.$$

$$\left. \times \bar{E}\left(\bar{r}'' \right) \right]$$
$$= \bar{E}\left(\bar{r} \right) \text{ for } \bar{r} \text{ in } V_0 \text{ of } (0,0,0)$$
$$= 0 \text{ for } \bar{r} \text{ in } V_1 \text{ of } (0,0,0) \tag{D8}$$

D.3. Lattice Dyadic Green's Function

The electric field is now shifted to (0, 0, 0) cell, and we then wrap up the summation of dyadic free space Green's function with phase shift into lattice dyadic Green's function.

$$\overline{\overline{G}}_P \left(\bar{r}, \bar{r}'' \right) = \sum_{\sigma} \overline{\overline{G}}_0 \left(\bar{r}, \bar{r}'' + \bar{R}_\sigma \right) \exp\left(i\bar{k}_i \cdot \bar{R}_\sigma \right) \tag{D9}$$

The simplified integral equation is

$$\oint_{S_B} dS' \left[i\omega\mu \overline{\overline{G}}_P \left(\bar{r}, \bar{r}' \right) \cdot \hat{n}' \times \bar{H}\left(\bar{r}' \right) + \nabla \times \overline{\overline{G}}_P \left(\bar{r}, \bar{r}' \right) \right.$$

$$\left. \cdot \hat{n}' \times \bar{E}\left(\bar{r}' \right) \right]$$
$$= \bar{E}\left(\bar{r} \right) \text{ for } \bar{r} \text{ in } V_0 \text{ of } (0,0,0)$$
$$= 0 \text{ for } \bar{r} \text{ in } V_1 \text{ of } (0,0,0) \tag{D10}$$

where we can also wrap up free space Green's function with phase shift for lattice Green's function g_P [15] to give the following lattice dyadic Green's function.

$$\overline{\overline{G}}_P \left(\bar{r}, \bar{r}'' \right) = \left(\overline{\overline{I}} + \frac{1}{k^2} \nabla\nabla \right) g_P \left(k, \bar{k}_i, \bar{r}, \bar{r}'' \right) \tag{D11}$$

Assuming inversion symmetry for $\bar{k}_i$ and $\bar{R}_s$.

$$g_P \left(k, \bar{k}_i, \bar{r} \right) = g_P \left(i\xi, \bar{k}_i, \bar{r} \right) - \frac{\xi^2 + k^2}{2\xi} \left(\frac{d}{d\xi} \right)$$

$$g_P \left(i\xi, \bar{k}_i, \bar{r} \right) + \frac{\left(\xi^2 + k^2 \right)^2}{8\xi} \left(\frac{d}{d\xi} \frac{1}{\xi} \frac{d}{d\xi} \right) g_P \left(i\xi, \bar{k}_i, \bar{r} \right)$$

$$+ \frac{\left(\xi^2 + k^2 \right)^3}{\Omega} \sum_s \exp\left(i\bar{k}_{is} \cdot \bar{r} \right)$$

$$\left[\frac{1}{\left(k_{is}^2 + \xi^2 \right)^3 - \left(k_{is}^2 - k^2 \right)} \right] \tag{D12}$$

where

$$g_P \left(i\xi, \bar{k}_i, \bar{r} \right) = \sum_s \frac{\exp\left(-\xi \left| \bar{r} - \bar{R}_s \right| \right)}{4\pi \left| \bar{r} - \bar{R}_s \right|} \exp\left(i\bar{k}_i \cdot \bar{R}_s \right) \tag{D13}$$

Note that $\bar{r}$ in $g_P(i\xi, \bar{k}_i, \bar{r})$ is for $\bar{r} - \bar{r}''$ using notation in $\overline{\overline{G}}_P(\bar{r}, \bar{r}'')$ for simplicity.

Without losing generality, we let $\bar{r}''$ be the origin. Then

$$\overline{\overline{G}}_P \left(\bar{r}, 0 \right) = \left(\overline{\overline{I}} + \frac{1}{k^2} \nabla\nabla \right) \sum_s \frac{\exp\left(-\xi \left| \bar{r} - \bar{R}_s \right| \right)}{4\pi \left| \bar{r} - \bar{R}_s \right|}$$

$$\exp\left(i\bar{k}_i \cdot \bar{R}_s \right) - \frac{\xi^2 + k^2}{2\xi} \left(\frac{d}{d\xi} \right) \left(\overline{\overline{I}} + \frac{1}{k^2} \nabla\nabla \right) \sum_s$$

$$\frac{\exp\left(-\xi \left| \bar{r} - \bar{R}_s \right| \right)}{4\pi \left| \bar{r} - \bar{R}_s \right|} \exp\left(i\bar{k}_i \cdot \bar{R}_s \right) + \frac{\left(\xi^2 + k^2 \right)^2}{8\xi}$$

$$\left(\frac{d}{d\xi} \frac{1}{\xi} \frac{d}{d\xi} \right) \left(\overline{\overline{I}} + \frac{1}{k^2} \nabla\nabla \right) \sum_s \frac{\exp\left(-\xi \left| \bar{r} - \bar{R}_s \right| \right)}{4\pi \left| \bar{r} - \bar{R}_s \right|}$$

$$\exp\left(i\bar{k}_i \cdot \bar{R}_s \right) + \frac{\left(\xi^2 + k^2 \right)^3}{\Omega} \sum_s \left[\frac{1}{\left(k_{is}^2 + \xi^2 \right)^3 \left(k_{is}^2 - k^2 \right)} \right]$$

$$\left(\overline{\overline{I}} - \frac{\bar{k}_{is} \bar{k}_{is}}{k^2} \right) \exp\left(i\bar{k}_{is} \cdot \bar{r} \right) \tag{D14}$$

For $\nabla \times \overline{\overline{G}}_P(\bar{r}, 0) \cdot \bar{a}$, we know $\nabla \times (\overline{\overline{I}} f(\bar{r})) \cdot \bar{a} = \nabla f(\bar{r}) \times \bar{a}$.

$$\nabla \times \overline{\overline{G}}_P \left(\bar{r}, 0 \right) \cdot \bar{a} = \nabla \sum_s \frac{\exp\left(i\alpha \left| \bar{r} - \bar{R}_s \right| \right)}{4\pi \left| \bar{r} - \bar{R}_s \right|} \exp\left(i\bar{k}_i \cdot \bar{R}_s \right)$$

$$\times \bar{a} - \frac{\xi^2 + k^2}{2\xi} \left(\frac{d}{d\xi} \right) \nabla \sum_s \frac{\exp\left(i\alpha \left| \bar{r} - \bar{R}_s \right| \right)}{4\pi \left| \bar{r} - \bar{R}_s \right|} \exp\left(i\bar{k}_i \cdot \bar{R}_s \right)$$

$$\times \bar{a} + \frac{\left(\xi^2 + k^2 \right)^2}{8\xi} \left(\frac{d}{d\xi} \frac{1}{\xi} \frac{d}{d\xi} \right) \nabla \sum_s \frac{exp\left(i\alpha \left| \bar{r} - \bar{R}_s \right| \right)}{4\pi \left| \bar{r} - \bar{R}_s \right|}$$

$$\exp\left(i\bar{k}_i \cdot \bar{R}_s \right) \times \bar{a} + \frac{\left(\xi^2 + k^2 \right)^3}{\Omega}$$

$$\nabla \sum_s \left[\frac{1}{\left(k_{is}^2 + \xi^2 \right)^3 \left(k_{is}^2 - k^2 \right)} \right] \exp\left(i\bar{k}_{is} \cdot \bar{r} \right) \times \bar{a} \tag{D15}$$

With the known surface field, $\hat{n}' \times \bar{E}(\bar{r}')$ and $\hat{n}' \times \bar{H}(\bar{r}')$ calculated from the eigen-vector, we can apply them to the integral equation using Huygen's principles shown here to calculate the electric fields outside the scatterer.

REFERENCES

[1] Joannopoulos, J. D., S. G. Johnson, J. N. Winn, and R. D. Meade, *Photonic Crystals: Molding the Flow of Light*, 2nd ed., Princeton University Press, 2008.

[2] Ozawa, T., H. M. Price, A. Amo, N. Goldman, M. Hafezi, L. Lu, M. C. Rechtsman, D. Schuster, J. Simon, O. Zilberberg, and I. Carusotto, "Topological photonics," *Reviews of Modern Physics*, Vol. 91, No. 1, 015006, Mar. 2019.

[3] Wang, Z., Y. D. Chong, J. D. Joannopoulos, and M. Soljačić, "Reflection-free one-way edge modes in a gyromagnetic photonic crystal," *Physical Review Letters*, Vol. 100, 013905, 2008.

[4] Yang, Z., F. Gao, X. Shi, X. Lin, Z. Gao, Y. Chong, and B. Zhang, "Topological acoustics," *Physical Review Letters*, Vol. 114, 114301, Mar. 2015.

[5] Ao, X., Z. Lin, and C. T. Chan, "One-way edge mode in a magneto-optical honeycomb photonic crystal," *Physical Review B*, Vol. 80, 033105, Jul. 2009.

[6] Tasolamprou, A. C., M. Kafesaki, C. M. Soukoulis, E. N. Economou, and T. Koschny, "Chiral topological surface states on a finite square photonic crystal bounded by air," *Physical Review Applied*, Vol. 16, 044011, 2021.

[7] Xi, X., B. Yan, L. Yang, Y. Meng, Z.-X. Zhu, J.-M. Chen, Z. Wang, P. Zhou, P. P. Shum, Y. Yang, *et al.*, "Topological antichiral surface states in a magnetic Weyl photonic crystal," *Nature Communications*, Vol. 14, 1991, 2023.

[8] Jin, J.-M., *The Finite Element Method in Electromagnetics*, 3rd ed., John Wiley & Sons, 2014.

[9] Zhao, R., G.-D. Xie, M. L. N. Chen, Z. Lan, Z. Huang, and W. E. I. Sha, "First-principle calculation of Chern number in gyrotropic photonic crystals," *Optics Express*, Vol. 28, No. 4, 4638–4649, 2020.

[10] Tsang, L., "Broadband calculations of band diagrams in periodic structures using the broadband Green's function with low wavenumber extraction (BBGFL)," *Progress In Electromagnetics Research*, Vol. 153, 57–68, 2015.

[11] Tsang, L. and S. Tan, "Calculations of band diagrams and low frequency dispersion relations of 2D periodic dielectric scatterers using broadband Green's function with low wavenumber extraction (BBGFL)," *Optics Express*, Vol. 24, No. 2, 945–965, 2016.

[12] Gao, R., L. Tsang, S. Tan, and T.-H. Liao, "Band calculations using broadband Green's functions and the KKR method with applications to magneto-optics and photonic crystals," *Journal of the Optical Society of America B*, Vol. 37, No. 12, 3896–3907, 2020.

[13] Gao, R., L. Tsang, S. Tan, and T.-H. Liao, "Broadband Green's function-KKR-Multiple Scattering Method for calculations of normalized band-field solutions in magneto-optics crystals," *Journal of the Optical Society of America B*, Vol. 38, No. 10, 3159–3171, 2021.

[14] Tsang, L., T.-H. Liao, and S. Tan, "Calculations of bands and band field solutions in topological acoustics using the broadband Green's function-KKR-Multiple Scattering Method," *Progress In Electromagnetics Research*, Vol. 171, 137–158, 2021.

[15] Tsang, L., T.-H. Liao, and S. Tan, "A fast computation method of bands and band field solutions of 3D periodic structures using broadband Green's Function-Multiple Scattering Theory," *Progress In Electromagnetics Research*, Vol. 176, 67–93, 2023.

[16] Tan, S. and L. Tsang, "Efficient broadband evaluations of lattice Green's functions via imaginary wavenumber components extractions," *Progress In Electromagnetics Research*, Vol. 164, 63–74, 2019.

[17] Foldy, L. L., "The multiple scattering of waves. I. General theory of isotropic scattering by randomly distributed scatterers," *Physical Review*, Vol. 67, 107–119, 1945.

[18] Lax, M., "Multiple scattering of waves," *Reviews of Modern Physics*, Vol. 23, No. 4, 287–310, 1951.

[19] Waterman, P. C. and R. Truell, "Multiple scattering of waves," *Journal of Mathematical Physics*, Vol. 2, No. 4, 512–537, 1961.

[20] Tsang, L., J. A. Kong, and R. T. Shin, *Theory of Microwave Remote Sensing*, Wiley-Interscience, 1985.

[21] Tsang, L., J. A. Kong, K.-H. Ding, and C. O. Ao, *Scattering of Electromagnetic Waves, Vol. 2: Numerical Simulations*, Wiley-Interscience, 2001.

[22] Korringa, J., "On the calculation of the energy of a Bloch wave in a metal," *Physica*, Vol. 13, No. 6-7, 392–400, 1947.

[23] Tsang, L., J. A. Kong, and K.-H. Ding, *Scattering of Electromagnetic Waves, Vol. 1: Theory and Applications*, Wiley Interscience, 2000.

[24] Wang, X., X.-G. Zhang, Q. Yu, and B. N. Harmon, "Multiple-scattering theory for electromagnetic waves," *Physical Review B*, Vol. 47, No. 8, 4161–4167, 1993.

[25] Kohn, W. and N. Rostoker, "Solution of the Schrödinger equation in periodic lattices with an application to metallic lithium," *Physical Review*, Vol. 94, 1111–1120, 1954.

[26] Kambe, K., "Theory of electron diffraction by crystals: I. Green's function and integral equation," *Zeitschrift für Naturforschung A*, Vol. 22, No. 4, 422–431, Apr. 1967.

[27] Gu, W., L. Tsang, A. Colliander, and S. Yueh, "Propagation of waves in vegetations using a hybrid method," *IEEE Transactions on Antennas and Propagation*, Vol. 69, No. 10, 6752–6761, Oct. 2021.

[28] Gu, W., L. Tsang, A. Colliander, and S. H. Yueh, "Multi-frequency full-wave simulations of vegetation using a hybrid method," *IEEE Transactions on Microwave Theory and Techniques*, Vol. 70, No. 1, 275–285, Jan. 2022.

[29] Tsang, L., T.-H. Liao, R. Gao, H. Xu, W. Gu, and J. Zhu, "Theory of microwave remote sensing of vegetation effects, soop and rough soil surface backscattering," *Remote Sensing*, Vol. 14, No. 15, 3640, 2022.

[30] Huang, H., L. Tsang, A. Colliander, R. Shah, X. Xu, and S. Yueh, "Multiple scattering of waves by complex objects using hybrid method of T-matrix and Foldy-Lax equations using vector spherical waves and vector spheroidal waves," *Progress In Electromagnetics Research*, Vol. 168, 87–111, 2020.

[31] Harrington, R. F., *Time-harmonic Electromagnetic Fields*, McGraw-Hill, 1961.

[32] Sarabandi, K., *Foundations of Applied Electromagnetics*, Michigan Publishing, 2022.